

Computing data for Levin-Wen with defects

Jacob C. Bridgeman¹ and Daniel Barter²

¹Perimeter Institute for Theoretical Physics, Waterloo, Ontario, Canada

²Mathematical Sciences Institute, Australian National University, Canberra, Australia

May 28, 2020

We demonstrate how to do many computations for doubled topological phases with defects. These defects may be 1-dimensional domain walls or 0-dimensional point defects.

Using $\text{Vec}(S_3)$ as a guiding example, we demonstrate how domain wall fusion and associators can be computed using generalized tube algebra techniques. These domain walls can be both between distinct or identical phases. Additionally, we show how to compute all possible point defects, and the fusion and associator data of these. Worked examples, tabulated data and Mathematica code are provided.

1 Introduction

Topological phases are of great interest in quantum information theory. By leveraging their topological nature, quantum information can be stored and manipulated in a manner which is protected against any local noise[1–4]. For such encodings to be useful in our attempts to build a quantum computer, it is necessary to find ways of implementing *universal sets* of logic gates.

Unfortunately, many of the simplest topological codes only allow limited gate sets to be implemented in a fault tolerant manner. On the other hand, some topological codes admit universal gate sets, but are incredibly challenging to engineer. Recently, a hybrid approach has been proposed[5]. This primarily relies on the (relatively) straightforward code for storage and manipulation, but included small ‘islands’ of a more powerful phase to leverage their computational power.

Hybrid schemes such as that described above, require information to be exchanged between codes. One way to achieve this directly in the material is to introduce *gapped domain walls* between the two phases in question. Once domain walls are introduced, either between identical or distinct codes, one can also introduce point-like defects on these domain walls. These defects can also be used to increase the computational power of the underlying codes[6–15]. The most famous example of this is the introduction of Majorana twists into the surface code[7, 9, 16]. The mathematical theory of symmetry defects is developed in Refs. [17–19]. In this work, we provide a computational framework for obtaining data associated to defects. This data is required when designing quantum computational schemes.

In this paper, we study the renormalization invariant properties of (2+1)D, long range entangled, doubled topological phases with defects. In particular, we study phases constructed from the symmetric group S_3 and its subgroups $\{0\}$, $\mathbb{Z}/2\mathbb{Z}$ and $\mathbb{Z}/3\mathbb{Z}$. These phases are often called *Kitaev quantum double phases* and were defined on the lattice in Ref. [1]. The corresponding quantum field theories were initially introduced by Dijkgraaf and Witten in Ref. [20]. Although our methods generalize, we focus on these models because our techniques are best illustrated by example, rather than a more abstract approach. As the smallest nonabelian group, S_3 is a natural example which realizes many of the complexities of the general case.

Much work has been done on the Kitaev quantum double phases corresponding to $\mathbb{Z}/2\mathbb{Z}$ and S_3 , for example Refs. [5, 21–27]. The $\mathbb{Z}/2\mathbb{Z}$ -phase is central to quantum information theory and quantum computing. Realizing the $\mathbb{Z}/2\mathbb{Z}$ phase is currently a major experimental effort because it can be used to build quantum memories[2–4]. When realized on the torus, it has 4 ground states which are topologically protected. The S_3 Kitaev quantum double phase is the simplest gapped phase which supports non-abelian anyons, hence is of central interest in quantum computing. Experimentally realizing non-abelian anyons is one of the central problems in topological quantum computing[28–32].

Jacob C. Bridgeman: jcbri@gmail.com, <https://jcbri.github.io>

Daniel Barter: danielbarter@gmail.com, <https://danielbarter.github.io>

Topological phases (of the kind we discuss) are parameterized by unitary modular tensor categories (UMTCs). Our work concerns UMTCs that arise as the *Drinfeld center* of a unitary fusion category \mathcal{C} . Although not all UMTCs are Drinfeld centers of fusion categories, for example, the (chiral) Fibonacci or (chiral) semion modes, there are many interesting UMTCs which are Drinfeld centers. For example, the category describing the low energy excitations of any Levin-Wen model[33] is a Drinfeld center. The fusion categories that arise in this paper are \mathbf{Vec} , $\mathbf{Vec}(\mathbb{Z}/2\mathbb{Z})$, $\mathbf{Vec}(\mathbb{Z}/3\mathbb{Z})$ and $\mathbf{Vec}(S_3)$ (defined below).

1.1 What is being computed in this work

This paper is a continuation of the work begun in Refs. [34–36]. In the current work, we generalize the methods developed there for $\mathbf{Vec}(\mathbb{Z}/p\mathbb{Z})$ to more general input (unitary) fusion categories, and provide code to compute essentially complete data on the defect theories. We focus on the example $\mathbf{Vec}(S_3)$, both to illustrate the methods, and to make more complete data available to researchers interested in universal quantum computation using ‘small’ topological phases. In particular, we show how the following data is computed. Let $\mathcal{A} \curvearrowright \mathcal{M} \curvearrowleft \mathcal{B}$ and $\mathcal{B} \curvearrowright \mathcal{N} \curvearrowleft \mathcal{C}$ be bimodule categories (domain walls). Then we compute:

- The Brauer-Picard fusion tables for such bimodules.
- The codimension 2 defects lying at the interface of \mathcal{M} and \mathcal{N} .
- The vertical fusion rules of these defects, including $\text{End}(\mathcal{M})$ as a special case.
- The associator for this fusion.
- The horizontal fusion of these defects.
- The ‘ O_3 ’ bimodule associator.

From a mathematical perspective, we are computing decomposition rules for relative tensor product and composition of bimodule functors. In an upcoming paper Ref. [37], we will provide a rigorous proof of this fact using a robust theory of skeletalization of fusion categories and their bimodules.

1.2 Key results

The key mathematical results of this work are as follows:

- Given a set of domain walls, how do they fuse (compute the Brauer-Picard tables).
- Given a set of domain walls, it is natural to ask if their twists can be treated as anyons. The obstruction to this is the O_3 and O_4 cohomology classes defined in Ref. [38].

Proposition 1. *Let I and G_1 be the invertible $\mathbf{Vec}(S_3)|\mathbf{Vec}(S_3)$ domain walls. Then the O_3 and O_4 obstructions vanishes for $\{I, G_1\}$.*

This result seems to be known in Ref. [18], but we have been unable to find the computation in the literature.

- If $\mathcal{C} \curvearrowright \mathcal{M}$ is a boundary to vacuum, then the binary interface defects on \mathcal{M} form a fusion category under vertical fusion called $\text{End}(\mathcal{M})$. If \mathcal{M} is indecomposable, then \mathcal{C} and $\text{End}(\mathcal{M})$ are Morita equivalent[39]. If we let $\mathcal{C} = \mathbf{Vec}(\mathbb{Z}/3\mathbb{Z} \times S_3)$ and $\mathcal{M} = Q_8$, then $\text{End}(Q_8)$ is a $\mathbb{Z}/3\mathbb{Z} \times \mathbb{Z}/3\mathbb{Z}$ Tambara-Yamagami category[40]. This establishes the following:

Proposition 2. *$\mathbf{Vec}(\mathbb{Z}/3\mathbb{Z} \times S_3)$ is Morita equivalent to the Tambara-Yamagami category $\mathcal{TY}(\mathbb{Z}/3\mathbb{Z} \times \mathbb{Z}/3\mathbb{Z}, \chi, 1)$, where $\chi((g_0, h_0), (g_1, h_1)) = \omega^{g_0 h_1 + h_0 g_1}$.*

To the best of our knowledge, previously this TY category was only known to be group-theoretical[41] (the associator on $\mathbf{Vec}(G)$ was unknown)¹.

¹After this preprint was released, we were made aware that this is a special case of Cor. 5.15 in Ref. [42]

1.3 Structure of the paper

This paper is structured as follows. In Section 2 we provide some definitions and mathematical preliminaries that are required for the remainder of the paper. In Section 3, we define all the domain walls which appear in this paper. In Section 4 we discuss some explicit examples of computations. In Section 4.4, we describe the O_3 and O_4 obstructions, and prove Proposition 1. In Section 5, we summarize.

At its heart, this paper is about explicit computations. In Appendix A we construct a $(2+\epsilon)$ dimensional defect TQFT, which is our main computational tool. In Appendix B, we tabulate defining data for all the domain walls which appear in this paper. Appendices C-E consist of tables of computed data. Only a small amount of what we can actually compute is included, and we have tried to only include data which hasn't previously appeared in the literature. Perhaps the most striking computation appears in Appendix F. We compute the associator for $\text{End}(Q_8)$, thereby proving Proposition 2. Code used for the computations in this paper is provided in the ancillary material[43].

2 Preliminaries

In this paper, we make extensive and careful use of a diagrammatic formalism. Diagrams fall into two classes, those with a gray textured background and those with a white background.

Diagrams with white backgrounds do not have a direct physical interpretation. They are simply a diagrammatic calculus used to describe tensor categories and module categories. This diagrammatic calculus, first popularized by Penrose in Ref. [44], is used because it is cumbersome to describe fusion categories using conventional mathematical notation. A diagram with a white background must be interpreted using the coordinate chart induced by the page on which it is drawn.

Diagrams with a gray background are to be interpreted physically. For example, compound defects (defined below) completely specify physical systems and are therefore depicted with a gray background. The ground states of a system described by such a gray diagram are the skein vectors described in Appendix A. The physical system (or state) specified by a diagram with a gray background is independent of coordinate chart. Diagrams with a gray background are closely related to the diagrammatic calculus used to describe *rigid* tensor categories in Ref. [45].

Definition 3 (Fusion category). A *tensor category* \mathcal{C} is a category \mathcal{C} equipped with a functor $- \otimes - : \mathcal{C} \otimes \mathcal{C} \rightarrow \mathcal{C}$, a natural isomorphism $(- \otimes -) \otimes - \cong - \otimes (- \otimes -)$ called the associator and a special object $1 \in \mathcal{C}$ which satisfy the pentagon equation and unit equations respectively. These can be found on Page 22 of Ref. [39]. If \mathcal{C} is semi-simple, using the string diagram notation as explained in Ref. [45], a vector α in $\mathcal{C}(a \otimes b, c)$ can be represented by a trivalent vertex:

$$\begin{array}{c} c \\ \swarrow \downarrow \searrow \\ a \quad b \end{array} . \quad (1)$$

If we choose bases for all the vector spaces $\mathcal{C}(a \otimes b, c)$ (the Hom spaces), then the associator can be represented as a tensor F , where

$$\begin{array}{c} d \\ \swarrow \quad \searrow \\ \alpha \quad \beta \\ \swarrow \quad \searrow \\ a \quad b \end{array} \quad e \quad c = \sum_{\mu\nu} F_{\alpha\beta}^{\mu\nu} \begin{array}{c} d \\ \swarrow \quad \searrow \\ \nu \quad \mu \\ \swarrow \quad \searrow \\ a \quad b \end{array} \quad f \quad c . \quad (2)$$

where $\alpha \in \mathcal{C}(a \otimes b, e)$, $\beta \in \mathcal{C}(e \otimes c, d)$, $\mu \in \mathcal{C}(b \otimes c, f)$ and $\nu \in \mathcal{C}(a \otimes f, d)$ are basis vectors.

A *fusion category* is a semi-simple rigid tensor category \mathcal{C} with a finite number of simple objects and a simple unit. An object is *simple* if there are no non-trivial sub-objects. *Semi-simple* means that every object in \mathcal{C} is a direct sum of simple objects. *Rigid* is a technical condition defined on Page 40 of Ref. [39] which implies that objects in \mathcal{C} have duals and they behave like duals in the category of vector spaces.

In Ref. [33], Levin and Wen defined a topological phase associated to any unitary fusion category \mathcal{C} . These are the phases of interest in this paper. All fusion categories considered in this work are assumed to be unitary.

Definition 4 ($\mathbf{Vec}(G)$). Let G be a finite group and V a vector space. A G -grading on V is a direct sum decomposition of $V = \oplus_{g \in G} V_g$. The fusion category $\mathbf{Vec}(G)$ is the category of G -graded (finite dimensional) vector spaces. The morphisms are linear maps which preserve the grading. The tensor product is define by

$$(V \otimes W)_k = \oplus_{gh=k} V_g \otimes W_h, \quad (3)$$

and the associator is trivial. The (isomorphism classes of) simple objects in $\mathbf{Vec}(G)$ are parameterized by $g \in G$, where g is synonymous with the 1 dimensional vector space in degree g . Using this notation, the tensor product can be written

$$g \otimes h = gh \quad (4)$$

without confusion. We can choose trivalent vertices

$$\begin{array}{c} gh \\ | \\ g \quad h \end{array} \quad (5)$$

such that

$$\begin{array}{c} ghk \\ / \quad \backslash \\ gh \quad k \\ / \quad \backslash \\ g \quad h \end{array} = \begin{array}{c} ghk \\ / \quad \backslash \\ g \quad hk \\ / \quad \backslash \\ g \quad h \end{array} \quad (6)$$

Definition 5 (Bimodule category). Let \mathcal{C}, \mathcal{D} be fusion categories. A *bimodule category* $\mathcal{C} \curvearrowright \mathcal{M} \curvearrowleft \mathcal{D}$ is a semi-simple category equipped with functors $- \triangleright - : \mathcal{C} \otimes \mathcal{M} \rightarrow \mathcal{M}$ and $- \triangleleft - : \mathcal{M} \otimes \mathcal{D} \rightarrow \mathcal{M}$ and three natural isomorphisms

$$- \triangleright (- \triangleright -) \cong (- \otimes -) \triangleright - \quad (7a)$$

$$(- \triangleleft -) \triangleleft - \cong - \triangleleft (- \otimes -) \quad (7b)$$

$$- \triangleright (- \triangleleft -) \cong (- \triangleright -) \triangleleft -. \quad (7c)$$

If we choose bases for the Hom spaces $\mathcal{M}(c \triangleright m, n)$ and $\mathcal{M}(m \triangleleft d, n)$, then these natural isomorphisms can be represented as tensors:

$$\begin{array}{c} n \\ | \\ \beta \\ p \\ \alpha \\ | \\ a \quad b \quad m \end{array} = \sum_{\mu\nu} L_{\alpha\beta}^{\mu\nu} \begin{array}{c} n \\ | \\ \mu \\ q \\ \nu \\ | \\ a \quad b \quad m \end{array}. \quad (8a)$$

$$\begin{array}{c} n \\ | \\ \beta \\ p \\ \alpha \\ | \\ a \quad m \quad b \end{array} = \sum_{\mu\nu} C_{\alpha\beta}^{\mu\nu} \begin{array}{c} n \\ | \\ \nu \\ q \\ \mu \\ | \\ a \quad m \quad b \end{array}, \quad (8b)$$

$$\begin{array}{c} n \\ | \\ \beta \\ p \\ \alpha \\ | \\ m \quad a \quad b \end{array} = \sum_{\mu\nu} R_{\alpha\beta}^{\mu\nu} \begin{array}{c} n \\ | \\ \nu \\ q \\ \mu \\ | \\ m \quad a \quad b \end{array}. \quad (8c)$$

Bimodule categories parameterize domain walls between the Levin-Wen phases[46–48]. We will therefore use the words *domain wall* and *bimodule* interchangeably.

Theorem 6. *There exists a $(2 + \epsilon)D$ defect TQFT which captures the renormalization invariant properties of all long range entangled, doubled 2D topological phases and their defects.*

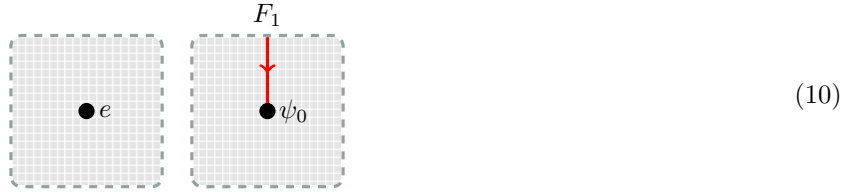
Theorem 6 is the main technical tool which facilitates the computations of interest in this paper. The TQFT is constructed in Appendix A. It is built from the tensors F, L, C, R and some other data related to rigid structures on fusion categories. It is a $(2+\epsilon)$ D theory because we can compute path integrals on cylinders, but not all 3-manifolds.

Definition 7 (Domain wall structure). Let Σ be an oriented surface and $D \subseteq \Sigma$ an embedded oriented 1-manifold transverse to the boundary of Σ such that $\partial D \subseteq \partial \Sigma$. Label each connected component of $\Sigma \setminus D$ with a unitary fusion category. Label each component of D with a bimodule between the adjacent fusion categories. We call the pair $D \subseteq \Sigma$ together with the face and edge labels a *domain wall structure*. A small open neighborhood in a domain wall structure looks something like



It is important to notice that the boundary components of Σ are not labeled with boundaries to vacuum. Therefore, a domain wall structure does not completely specify a physical system (it has a mixed gray/white background). In order to get a physical system, the boundary components of Σ must be filled in with point defects. We stress that a system with a boundary would involve a *filled* region labeled by **Vec**. The term domain wall structure first appeared in Ref. [36]. Surfaces decorated with domain walls play a central role in the theory of defect TQFTs. The survey Ref. [49] by Carqueville is a great introduction to this field.

Definition 8 (Point defect). In order to define a physical system from a domain wall structure Σ , the holes in Σ must be resolved. *Point defects* are the “particles” used to fill these holes. As is often the case in quantum field theory, the particle types are parameterized by representations of a local observable algebra. We define the local observable algebra in Definition 22 in Appendix A. Some of the point defects of interest in this paper will be familiar. For example anyons, which parameterize the low energy excitations for a long range entangled topological phase, and twists which terminate invertible domain walls are both examples of point defects.



In this paper, we are also interested in several other types of point defects. *Binary interface defects* are the particles which interface between two domain walls



Point defects were first defined by Morrison and Walker in Ref. [50], where they are called *sphere modules*. Point defects in the $\mathbf{Vec}(\mathbb{Z}/p\mathbb{Z})$ phase were studied in Refs. [35, 36].

Definition 9 (Compound defect). A *Compound Defect* is a domain wall structure Σ together with point defects

to resolve all the holes in Σ .

$$(12)$$

Compound defects are a complete specification of a physical system. The ground states $Z(\Sigma)$ of this system are spanned by the skein vectors which can be drawn on top of the system as described in Appendix A. Two skein vectors are equivalent if one can be transformed into the other using local relations.

Definition 10 (Generalized Levin-Wen lattice models). Let Σ be a compound defect. We can define a Levin-Wen[33] type model as follows: The local degrees of freedom on the edges are simple objects in the labeling bimodule. The local degrees of freedom on the vertices are vectors in the corresponding point defect representation. Let H be the global Hilbert space. The Hamiltonian is a commuting projector Hamiltonian with two types of terms, vertex terms P_v and face terms P_f . The vertex terms project onto the states where the object labels for the vertex states match the local degrees of freedom on the edges. The face terms apply the operator

$$P_f = \frac{1}{\dim(\mathcal{C})} \sum_{a \in \mathcal{C}} \dim(a) a \quad (13)$$

depicted in equation Eqn. 75. The ground states of this model are

$$\{\psi | P_v \psi = \psi, P_f \psi = \psi\} \cong H / \mathbb{C}\{\psi - P_v \psi, \psi - P_f \psi\} \cong Z(\Sigma) \quad (14)$$

The projection onto the ground states in Eqn. 14 is

$$\prod_f P_f \prod_v P_v. \quad (15)$$

For this reason, we can write a Levin-Wen ground state as

$$|\psi\rangle \propto \left| \begin{array}{c} \text{empty box} \end{array} \right\rangle + \dim(a) \left| \begin{array}{c} \text{loop } a \end{array} \right\rangle + \dim(a)\dim(b) \left| \begin{array}{c} \text{two loops } a, b \end{array} \right\rangle + \dim(c) \left| \begin{array}{c} \text{loop } c \end{array} \right\rangle + \dots \quad (16)$$

In this paper we shall use both the skein theoretic description of ground states and the loop superposition description of ground states interchangeably. We will always surround the loop superposition description with bra-kets.

Definition 11 (Renormalization). A compound defect can be renormalized to a point defect:

$$(17)$$

The point defects W_i are determined by taking the space of skein vectors supported on the left hand compound defect and looking how they transform with respect to the local observable algebra.

The following four examples of renormalization are the main focus of this paper:

Definition 12 (Domain wall fusion). We can horizontally fuse domain walls by horizontally concatenating and then renormalizing

$$(18)$$

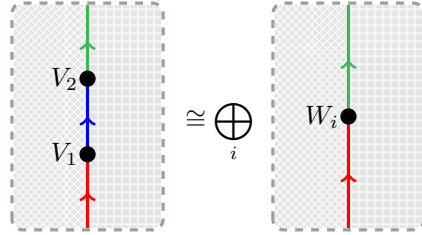
We call the fusion ring for domain walls the *Brauer-Picard ring* (BPR). Computing the BPR for $\mathbf{Vec}(\mathbb{Z}/p\mathbb{Z})$ was the subject of Ref. [34].

Using the inflation trick from Definition 30 in Appendix A, we can encode these domain wall fusions as point defects



$$(19)$$

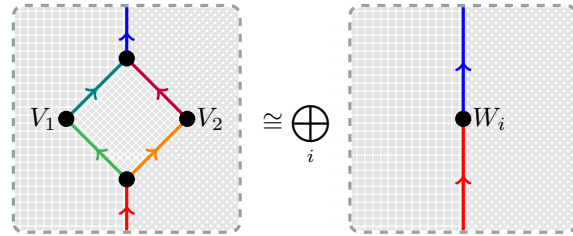
Definition 13 (Vertical fusion).



$$(20)$$

The defects interfacing between the domain wall \mathcal{M} and itself form a fusion category $\text{End}(\mathcal{M})$. The components of the isomorphism Eqn. 20 are trivalent vertices in $\text{End}(\mathcal{M})$ and we can compute the associator for $\text{End}(\mathcal{M})$ as described in Definition 31.

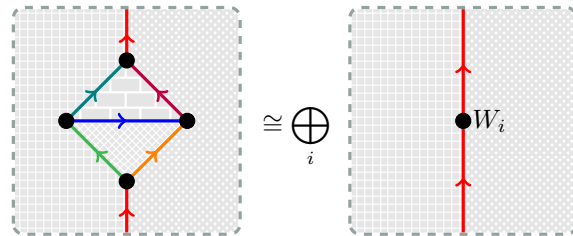
Definition 14 (Horizontal fusion).



$$(21)$$

where the trivalent point defects are those which encode the domain wall fusions as described in Definition 8.

Definition 15 (Associators).



$$(22)$$

All the trivalent point defects are encoding domain wall fusions.

Definition 16 (S_3 as a semi-direct product). It is well known that $S_3 \cong \mathbb{Z}/2\mathbb{Z} \ltimes \mathbb{Z}/3\mathbb{Z}$ where the involution on $\mathbb{Z}/3\mathbb{Z}$ is multiplication by 2. Throughout this paper, S_3 plays an important role and we use the semi-direct product presentation of S_3 because it is more amenable to computer implementation. In this representation, multiplication is given by

$$(a_0, b_0) \cdot (a_1, b_1) = (a_0 + a_1, (1 + a_1)b_0 + b_1), \quad (23)$$

where the first entry is taken modulo 2 and the second modulo 3. One caveat of this notation is that sometimes you need to be careful about applying the “obvious” rules of arithmetic like associativity and distributivity.

3 Domain Wall Definitions

In this section, we briefly discuss the domain walls (bimodule categories) that occur in this paper. Recall from Chapter 7 of Ref. [39] that $\mathbf{Vec}(G_1)|\mathbf{Vec}(G_2)$ bimodules are classified by a subgroup $M \leq G_1 \times G_2^{\text{op}}$ and a 2-cocycle

$$\omega \in H^2(M, U(1)) \quad (24)$$

$$\cong H^2(G_1 \times G_2^{\text{op}}, \text{maps}(G_1 \times G_2^{\text{op}}/M, U(1))) \quad (25)$$

up to conjugation. This defining data is provided in Appendix B. Where these domain walls have occurred in the literature, we have attempted to be consistent with already established names. In many cases, we have named corresponding $\mathcal{C}|\mathcal{D}$ and $\mathcal{D}|\mathcal{C}$ bimodules with the same label. Which version of the bimodule is being discussed can be easily inferred from context.

Simple objects in the bimodule category are labeled by cosets of M . The cocycle ω in Eqn. 24 does not directly give the associators of the fusion category action. One way to see this is that the associator is defined for a triple $(g_1, g_2, m) \in G_1 \times G_2^{\text{op}} \times (G_1 \times G_2^{\text{op}}/M)$, whereas Eqn. 24 has domain $M \times M$. The associator is obtained via the isomorphism to Eqn. 25. An implementation of this isomorphism is given by Tyler Lawson in Ref. [51]. For all the bimodules considered in this paper, a gauge can be chosen such that the left and right associators are trivial. We have used the following equations for $\mathbf{Vec}(S_3)|\mathbf{Vec}(S_3)$ domain walls

$$A_{2,1} : \Omega((a, b), m, (c, d)) = (-1)^{ac} \quad (26a)$$

$$A_{3,1} : \Omega((a, b), m, (c, d)) = \omega^{(1+c)bd(-1)^{\lfloor m/2 \rfloor}}, m \in \{1, 2, 3, 4\} \quad (26b)$$

$$D_{R,1} : \Omega((a, b), m, (c, d)) = (-1)^{ac} \quad (26c)$$

$$D_{L,1} : \Omega((a, b), m, (c, d)) = (-1)^{ac} \quad (26d)$$

$$G_1 : \Omega((a, b), m, (c, d)) = \omega^{(1+c)bd(m+1)}, m \in \{0, 1\} \quad (26e)$$

$$F_1 : \Omega((a, b), *, (c, d)) = (-1)^{ac}, \quad (26f)$$

with all other associators being trivial. The gauge choices for other bimodules can be found in the code provided in the ancillary material[43].

4 Examples

In this section, we discuss some interesting example computations. This serves to both show how calculations are done, and to provide some physical interpretation for the results.

The computations performed in this paper are very similar to those in Refs. [34–36], and we refer the reader to those papers for more examples. Due to the increased complexity of $\mathbf{Vec}(S_3)$, the computations here require computer assistance[43].

4.1 Domain wall fusion

To compute the result of domain wall fusion, we use the algorithm described in Definition 29. Extensive examples are provided in Ref. [34] for the $\mathbf{Vec}(\mathbb{Z}/p\mathbb{Z})$ case. We therefore only provide two examples here, and refer the reader to the previous work for more details.

4.1.1 $G_1 \otimes_{\mathbf{Vec}(S_3)} G_1$

The first step in computing the decomposition of $G_1 \otimes_{\mathbf{Vec}(S_3)} G_1$ is to construct the Karoubi envelope of the ladder category (defined in Def. 29). The trivalent vertices for G_1 are

$$\begin{array}{c} \text{Diagram 1: A trivalent vertex with three incoming lines labeled } (a, b), m, (c, d) \text{ and one outgoing line labeled } m+a+c. \end{array} = \omega^{(1+c)bd(1+m)} \begin{array}{c} \text{Diagram 2: A trivalent vertex with three incoming lines labeled } (a, b), m, (c, d) \text{ and one outgoing line labeled } m+a+c. \end{array}, \quad (27)$$

with $m \in \{0, 1\}$. To construct the Karoubi envelope, we need to construct idempotent ladder diagrams

$$(28)$$

For such a diagram to be an idempotent, it must be the case that $x = 0$. Diagrams which can be related by multiplying by a general ladder diagram are isomorphic in the Ladder category[34], so it is sufficient to consider diagrams of the form

$$(29)$$

These diagrams form the group algebra $\mathbb{C}[\mathbb{Z}/3\mathbb{Z}]$, so the primitive idempotents are

$$X_{m,\alpha} := \frac{1}{3} \sum_y \omega^{\alpha y} \quad (30)$$

The left and right trivalent vertices are skein vectors that absorb these idempotents on the top and bottom. Being careful with the associator, one can check that in this case the vertices are

$$(31)$$

$$(32)$$

It is straightforward to verify that the associator is trivial. From this, we obtain

$$G_1 \otimes_{\mathbf{Vec}(S_3)} G_1 \cong I. \quad (33)$$

4.1.2 Interpreting $\mathcal{M} \otimes_{\mathcal{C}} \mathcal{N} = \mathcal{P} + \mathcal{Q}$

In the Brauer-Picard tables of Appendix C, there are instances of domain wall fusions of the kind

$$\mathcal{M} \otimes_{\mathcal{C}} \mathcal{N} = \mathcal{P} + \mathcal{Q}. \quad (34)$$

We now provide a physical interpretation of this result. For concreteness, we will consider the fusion of K_4 walls. The fusion for these domain walls is

$$K_4 \otimes_{\mathbf{Vec}(\mathbb{Z}/2\mathbb{Z})} K_4 = I_2 \quad (35)$$

$$K_4 \otimes_{\mathbf{Vec}(S_3)} K_4 = T^{\mathbb{Z}/2\mathbb{Z}} + X_1^{\mathbb{Z}/2\mathbb{Z}}. \quad (36)$$

We define three domain wall structures on the cylinder $\mathbb{R} \times S^1$:

$$\Sigma_{X_1} = \begin{array}{c} \text{Diagram: A rectangle with a green vertical line labeled } X_1 \text{ in the center. Arrows on the top and bottom edges point to the right.} \end{array} \quad (37a)$$

$$\Sigma_T = \begin{array}{c} \text{Diagram: A rectangle with a blue vertical line labeled } T \text{ in the center. Arrows on the top and bottom edges point to the right.} \end{array} \quad (37b)$$

$$\Sigma_{K_4, K_4} = \begin{array}{c} \text{Diagram: A rectangle with two red vertical lines labeled } K_4 \text{ on the left and right. Arrows on the top and bottom edges point to the right.} \end{array} \quad (37c)$$

The ground states on Σ_{X_1} and Σ_T are given respectively by

$$|\psi_a\rangle = \left| \begin{array}{c} \text{Diagram: Green line with a small circle on the left} \end{array} \right\rangle + \left| \begin{array}{c} \text{Diagram: Green line with a small circle on the right} \end{array} \right\rangle + \left| \begin{array}{c} \text{Diagram: Green line with a small circle on the left and a larger circle on the right} \end{array} \right\rangle + \left| \begin{array}{c} \text{Diagram: Green line with a small circle on the right and a larger circle on the left} \end{array} \right\rangle + \dots \quad (38a)$$

$$|\psi_{a,b}\rangle = \left| \begin{array}{c} \text{Diagram: Blue line with a small circle on the left} \end{array} \right\rangle + \left| \begin{array}{c} \text{Diagram: Blue line with a small circle on the right} \end{array} \right\rangle + \left| \begin{array}{c} \text{Diagram: Blue line with a small circle on the left and a larger circle on the right} \end{array} \right\rangle + \left| \begin{array}{c} \text{Diagram: Blue line with a small circle on the right and a larger circle on the left} \end{array} \right\rangle + \dots \quad (38b)$$

The logical operator for both Σ_{X_1} and Σ_T is wrapping a pair of m anyons around the cylinder. In the X_1 case, this flips the index. In the T case, performing the operation to the left (resp right) of the domain wall flips the left (right) index. We have an isomorphism of ground spaces

$$Z(\Sigma_{X_1}) \oplus Z(\Sigma_T) \cong Z(\Sigma_{K_4, K_4}). \quad (39)$$

The isomorphism is given locally by the following six rules:

$$\begin{array}{c} \text{Diagram: Green line labeled } X_1 \text{ with index } a \end{array} \mapsto \begin{array}{c} \text{Diagram: Two red lines labeled } K_4 \text{ with indices } (0,0) \text{ and } (a,0) \end{array} \quad (40a)$$

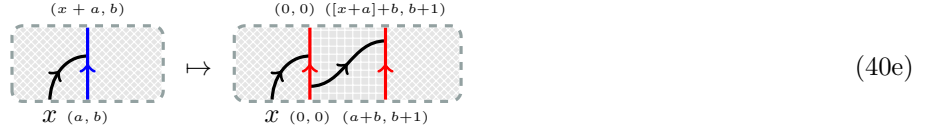
$$\begin{array}{c} \text{Diagram: Blue line labeled } T \text{ with index } (a,b) \end{array} \mapsto \begin{array}{c} \text{Diagram: Two red lines labeled } K_4 \text{ with indices } (0,0) \text{ and } (a+b, 1+b) \end{array} \quad (40b)$$

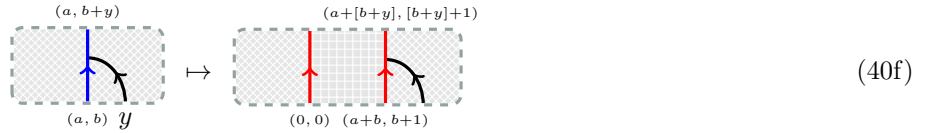
$$\begin{array}{c} \text{Diagram: Green line with index } x+a \text{ and a black arc from } x \text{ to } a \end{array} \mapsto \begin{array}{c} \text{Diagram: Two red lines with indices } (0,0) \text{ and } (x+a,0) \text{ and a black arc from } x \text{ to } (x,0) \end{array} \quad (40c)$$

$$\begin{array}{c} \text{Diagram: Green line with index } a+y \text{ and a black arc from } a \text{ to } y \end{array} \mapsto \begin{array}{c} \text{Diagram: Two red lines with indices } (0,0) \text{ and } (a+y,0) \text{ and a black arc from } (a,0) \text{ to } y \end{array} \quad (40d)$$

$\otimes \mathbf{Vec}(S_3)$	σ	$B\sigma$	$C\sigma$	ρ	$B\rho$	$C\rho$
σ	$A + G$	$B + G$	$C + F + H$	E	D	$D + E$
$B\sigma$	$B + G$	$A + G$	$C + F + H$	D	E	$D + E$
$C\sigma$	$C + F + H$	$C + F + H$	$A + B + C + F + 2G + H$	$D + E$	$D + E$	$2D + 2E$
ρ	E	D	$D + E$	$A + H$	$B + H$	$C + F + G$
$B\rho$	D	E	$D + E$	$B + H$	$A + H$	$C + F + G$
$C\rho$	$D + E$	$D + E$	$2D + 2E$	$C + F + G$	$C + F + G$	$A + B + C + F + G + 2H$

Table 1: Fusion rules for twists





4.1.3 Factoring domain walls

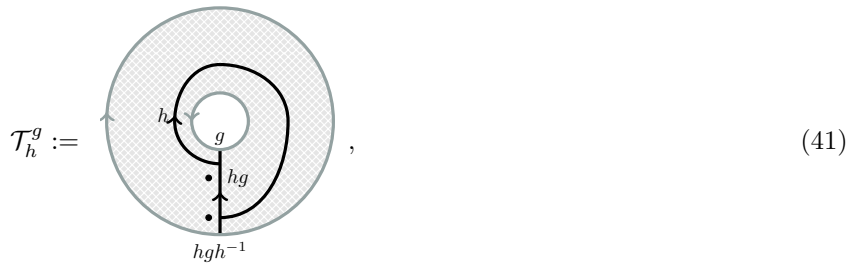
As observed in Ref. [34], many of the $\mathbf{Vec}(S_3)|\mathbf{Vec}(S_3)$ domain walls are noninvertible. From the BPR table 9, we see that there are only 2 invertible walls, with a $\mathbb{Z}/2\mathbb{Z}$ fusion rule. All other domain walls ‘factor through’ a smaller intermediate phase. The full set of (generalized) BPR tables are presented in Appendix C, we obtain physical interpretations for all bimodules. For example the $\mathbf{Vec}(S_3)|\mathbf{Vec}(S_3)$ wall named T is actually a pair of \mathcal{A}_1 boundaries separated by a strip of vacuum, just like the $T^{\mathbb{Z}/2\mathbb{Z}}$ in Table 20. Similar physical interpretations can be obtained for all walls.

4.2 Codimension 2 defects

We now discuss the excitations that live on domain walls. For the case of $\mathbf{Vec}(\mathbb{Z}/p\mathbb{Z})$, more examples can be found in Refs. [35, 36].

4.2.1 Finding point defects

The first task is to find the possible point defects. We describe this process for the special case of binary interface defects (BIDs), as defined in Eqn. 11. In particular, consider the case where $\mathcal{M} = \mathcal{M} = I$ (I defined in Table 5). The BIDs are labeled by representations of the annular category (in this case, this is the *tube algebra* [25, 26, 52]). A basis for the morphisms $g \rightarrow hgh^{-1}$ is



which compose as

$$\mathcal{T}_k^{hgh^{-1}} \mathcal{T}_h^g = \mathcal{T}_{kh}^g. \quad (42)$$

The first step in computing the representations of this category is to find the Karoubi envelope. This amounts to finding primitive idempotents in endomorphism algebras. By first identifying the h for which $g = hgh^{-1}$, and then

finding primitive idempotents for each matrix algebra, a simple computation shows that the isomorphism classes of simple objects in the Karoubi envelope are represented by

$$A = \frac{1}{6} \left(\mathcal{T}_{(0,0)}^{(0,0)} + \mathcal{T}_{(0,1)}^{(0,0)} + \mathcal{T}_{(0,2)}^{(0,0)} + \mathcal{T}_{(1,0)}^{(0,0)} + \mathcal{T}_{(1,1)}^{(0,0)} + \mathcal{T}_{(1,2)}^{(0,0)} \right) \quad (43a)$$

$$B = \frac{1}{6} \left(\mathcal{T}_{(0,0)}^{(0,0)} + \mathcal{T}_{(0,1)}^{(0,0)} + \mathcal{T}_{(0,2)}^{(0,0)} - \mathcal{T}_{(1,0)}^{(0,0)} - \mathcal{T}_{(1,1)}^{(0,0)} - \mathcal{T}_{(1,2)}^{(0,0)} \right) \quad (43b)$$

$$C = \frac{1}{3} \left(\mathcal{T}_{(0,0)}^{(0,0)} - \mathcal{T}_{(0,1)}^{(0,0)} - \mathcal{T}_{(1,0)}^{(0,0)} + \mathcal{T}_{(1,1)}^{(0,0)} \right) \quad (43c)$$

$$D = \frac{1}{2} \left(\mathcal{T}_{(0,0)}^{(1,0)} + \mathcal{T}_{(1,0)}^{(1,0)} \right) \quad (43d)$$

$$E = \frac{1}{2} \left(\mathcal{T}_{(0,0)}^{(1,0)} - \mathcal{T}_{(1,0)}^{(1,0)} \right) \quad (43e)$$

$$F = \frac{1}{3} \left(\mathcal{T}_{(0,0)}^{(0,1)} + \mathcal{T}_{(0,1)}^{(0,1)} + \mathcal{T}_{(0,2)}^{(0,1)} \right) \quad (43f)$$

$$G = \frac{1}{3} \left(\mathcal{T}_{(0,0)}^{(0,1)} + \omega \mathcal{T}_{(0,1)}^{(0,1)} + \omega^2 \mathcal{T}_{(0,2)}^{(0,1)} \right) \quad (43g)$$

$$H = \frac{1}{3} \left(\mathcal{T}_{(0,0)}^{(0,1)} + \omega^2 \mathcal{T}_{(0,1)}^{(0,1)} + \omega \mathcal{T}_{(0,2)}^{(0,1)} \right), \quad (43h)$$

where $\omega = \exp(\frac{2\pi i}{3})$.

Given these idempotents, the full representation can be constructed as described in Appendix A. The bimodule I is actually $\mathbf{Vec}(S_3)$ as a $\mathbf{Vec}(S_3)$ bimodule, and these representations describe the anyons of the theory.

4.2.2 Vertical fusion

Once we have obtained representations of point defects, we can compute more interesting properties of these excitations such as their fusion. In the case of vertical fusion, this is particularly straightforward. By examining how tubes act on the compound defect, we can obtain an explicit isomorphism to indecomposable point defects. For a triple compound defect, this isomorphism can be formed in two distinct ways as shown in Eqns. 91a-91b. The change of basis between these two families of isomorphisms gives the associator for $\text{End}(\mathcal{M})$. An explicit example is given in Appendix F.

4.2.3 Fusion of twists

One of the most studied domain wall excitations are termination points of invertible domain walls [7, 9, 13, 14, 17, 18, 26]. Commonly referred to as twists, these excitations are of interest for quantum computation [7, 9, 16]. For the only nontrivial invertible domain wall for $\mathbf{Vec}(S_3)$, the horizontal fusion rules for twists is shown in Table 1. From this table, we see that there are two kinds of ‘bare’ twist that cannot be interchanged by the action of anyons (the action is shown in Table 17).

In Ref. [18], it was conjectured that for a twist t , both $t \times t = A + G$ and $t \times t = A + H$ should occur. From Table 1, we see that this is indeed the case.

4.3 Logical operations on the toric code

The Toric code is one of the most famous examples in quantum information theory. Consider the Levin-Wen model for $\mathbf{Vec}(\mathbb{Z}/2\mathbb{Z})$ on the torus Σ . This system has a 4 dimensional ground space:

$$\mathbb{C} \left\{ \begin{array}{c} \text{[Diagram 1]} , \text{[Diagram 2]} , \text{[Diagram 3]} , \text{[Diagram 4]} \end{array} \right\} \quad (44)$$

Two types of logical operations often discussed for this model are the Dehn twists and the anyon loop operators. Using the tools developed in this paper, we can compute how these operations interact with each other and deduce the group of logical operators which they generate. The mapping class group of the torus, $\text{SL}(2, \mathbb{Z})$, is generated by two Dehn twists. The first cuts the torus along a horizontal loop (in our presentation), rotates a boundary circle

by 2π and then glues the cylinder back into a torus. This Dehn twist acts as the matrix

$$\begin{bmatrix} 1 & 0 & 0 & 0 \\ 0 & 1 & 0 & 0 \\ 0 & 0 & 0 & 1 \\ 0 & 0 & 1 & 0 \end{bmatrix} \quad (45)$$

We can think of the torus as $S^1 \times S^1$. The second Dehn twist swaps the factors and acts by the matrix

$$\begin{bmatrix} 1 & 0 & 0 & 0 \\ 0 & 0 & 1 & 0 \\ 0 & 1 & 0 & 0 \\ 0 & 0 & 0 & 1 \end{bmatrix} \quad (46)$$

The reader is most likely familiar with these Dehn twists acting via the T and S matrices of $Z(\mathbf{Vec}(\mathbb{Z}/2\mathbb{Z}))$ respectively. If we conjugate by

$$\begin{bmatrix} 1/2 & 1/2 & 0 & 0 \\ 1/2 & -1/2 & 0 & 0 \\ 0 & 0 & 1/2 & 1/2 \\ 0 & 0 & 1/2 & -1/2 \end{bmatrix} \quad (47)$$

which is the change of basis matrix from the skein basis to the basis which represents anyon flux through the center of the torus, we get

$$\begin{bmatrix} 1 & 0 & 0 & 0 \\ 0 & 1 & 0 & 0 \\ 0 & 0 & 1 & 0 \\ 0 & 0 & 0 & -1 \end{bmatrix} \quad \frac{1}{2} \begin{bmatrix} 1 & 1 & 1 & 1 \\ 1 & 1 & -1 & -1 \\ 1 & -1 & 1 & -1 \\ 1 & -1 & -1 & 1 \end{bmatrix} \quad (48)$$

respectively, as expected. To compute the anyon loop operators in the skein basis, we need to describe the anyon braidings, defined in Appendix A, for e and m . The e particle doesn't leave a trail as it propagates through the material, but when it crosses a string, the state gets multiplied by -1 . The m particle leaves a trail as it propagates, but doesn't pick up a phase when it crosses a string. A horizontal m loop acts via the matrix

$$\begin{bmatrix} 0 & 1 & 0 & 0 \\ 1 & 0 & 0 & 0 \\ 0 & 0 & 0 & 1 \\ 0 & 0 & 1 & 0 \end{bmatrix}. \quad (49)$$

Therefore, in the skein basis, every permutation matrix in S_4 is a logical operator. A horizontal e loop acts via the matrix

$$\begin{bmatrix} 1 & 0 & 0 & 0 \\ 0 & 1 & 0 & 0 \\ 0 & 0 & -1 & 0 \\ 0 & 0 & 0 & -1 \end{bmatrix}. \quad (50)$$

By conjugating with our permutation operators, we get a logical operator for each element of

$$(\mathbb{Z}/2\mathbb{Z})^3 \cong \{(a, b, c, d) \in (\mathbb{Z}/2\mathbb{Z})^4 | a + b + c + d = 0\} \quad (51)$$

The full group of logical operators generated by Dehn twists and anyon loops is isomorphic to $S_4 \ltimes (\mathbb{Z}/2\mathbb{Z})^3$.

4.4 Bimodule associators and obstructions

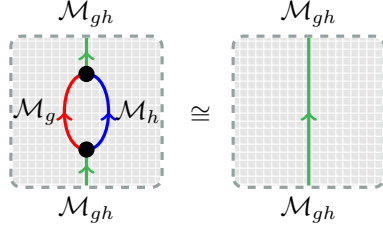
We now discuss the bimodule associators. For $\mathbf{Vec}(\mathbb{Z}/p\mathbb{Z})$, example computations can be found in Ref. [36].

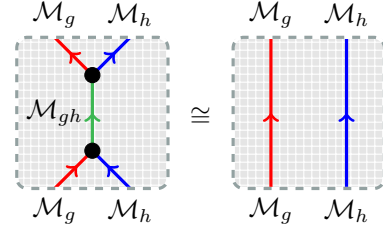
Suppose that we have a fusion category \mathcal{C} , a finite group G , a family of \mathcal{C} - \mathcal{C} bimodules $\{\mathcal{M}_g\}_{g \in G}$ and bimodule isomorphisms $\mathcal{M}_g \otimes_{\mathcal{C}} \mathcal{M}_h \cong \mathcal{M}_{gh}$. We present each of these bimodule isomorphisms as a pair of point defects:



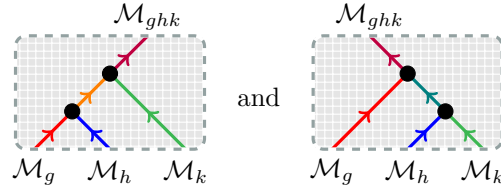
$$\quad (52)$$

which satisfy the following renormalization equations:

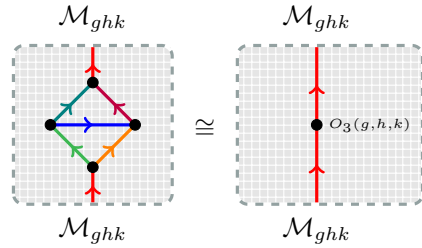

(53a)


(53b)

There are two obstructions for $\oplus_{g \in G} \mathcal{M}_g$ to form a tensor category. Firstly, it need not be the case that


(54)

are isomorphic representations of the 4-bimodule annular category. The obstruction to such an isomorphism existing is the following defect


(55)

as explained in Ref. [38], $O_3(g, h, k)$ is a cohomology class in $H^3(G, Z)$ where Z is the group of invertible anyons in $Z(\mathcal{C})$. If O_3 vanishes, then we can choose an isomorphism $\alpha_{g,h,k}$ between the two annular category representations in equation Eqn. 54. Secondly, there is no reason that the associator $\alpha_{g,h,k}$ satisfies the pentagon equation. The obstruction to this is called O_4 and as explained in Ref. [38], lives in $H^4(G, U(1))$. Since the loop space of $U(1)$ is homotopy equivalent to \mathbb{Z} , we have $H^4(G, U(1)) \cong H^5(G, \mathbb{Z})$.

In this paper, we are primarily interested in the case where $\mathcal{C} = \mathbf{Vec}(S_3)$, $G = \mathbb{Z}/2\mathbb{Z}$, and $\mathcal{M}_1 = G_1$. The group of invertible anyons in the $\mathbf{Vec}(S_3)$ phase is $\mathbb{Z}/2\mathbb{Z}$, so we have

$$O_3 \in H^3(\mathbb{Z}/2\mathbb{Z}, \mathbb{Z}/2\mathbb{Z}) \cong \mathbb{Z}/2\mathbb{Z} \quad (56)$$

$$O_4 \in H^4(\mathbb{Z}/2\mathbb{Z}, U(1)) \cong H^5(\mathbb{Z}/2\mathbb{Z}, \mathbb{Z}) = 0. \quad (57)$$

Therefore, it is not obvious that the O_3 obstruction vanishes. We have explicitly computed the O_3 obstruction in this case and it is zero. The O_4 obstruction vanishes trivially.

5 Remarks

In this work, we have studied doubled topological phases and their defects. We have shown how various data, including fusion and associators can be computed by evaluating *compound defects* in topological phases. We have

utilized these techniques (in a fully automated manner) to compute this data for $\mathbf{Vec}(\mathbb{Z}/p\mathbb{Z})$ and $\mathbf{Vec}(S_3)$, and interfaces between these.

Although we have specialized to $\mathbf{Vec}(G)$ in this work, the techniques described work more generally. Apart from the computational complexity, there is no obstruction to applying these algorithms to general fusion categories. The main challenge in that case is finding the bimodule categories, which we take as input data. It would be valuable to develop algorithms to find the data associated to these bimodules, beyond brute force solving of coherence equations.

From a quantum computational perspective, one of the most useful applications of this work is to study the ‘color code’ (the phase described by the fusion category $\mathbf{Vec}(\mathbb{Z}/2\mathbb{Z} \times \mathbb{Z}/2\mathbb{Z})$) [8, 53]. This category has 270 bimodules, so a computational approach, such as the one described here, is necessary. Since the color code supports transversal Clifford gates, generalizations of the universal hybrid scheme described in Ref. [5] to this code may prove important for topological quantum computation.

Although the cohomology group is nontrivial, we have shown the O_3 obstruction for $\mathbf{Vec}(S_3)$ vanishes. It would be interesting to study a case where this obstruction is nontrivial. The explicit nature of the computations performed here may shed light on when this is expected to occur.

Acknowledgments

This work is supported by the Australian Research Council (ARC) via Discovery Project “Subfactors and symmetries” DP140100732 and Discovery Project “Low dimensional categories” DP16010347. This research was supported in part by Perimeter Institute for Theoretical Physics. Research at Perimeter Institute is supported in part by the Government of Canada through the Department of Innovation, Science and Economic Development Canada and by the Province of Ontario through the Ministry of Economic Development, Job Creation and Trade. Many of the ideas presented here were first suggested to us by Corey Jones. This paper wouldn’t be possible without him. We thank Christopher Chubb for his comments on the manuscript.

References

- [1] A. Y. Kitaev, Fault-tolerant quantum computation by anyons, [Annals of Physics](#) **303**, 2, [arXiv:quant-ph/9707021](#) (2003).
- [2] E. Dennis, A. Kitaev, A. Landahl, and J. Preskill, Topological quantum memory, [Journal of Mathematical Physics](#) **43**, 4452, [arXiv:quant-ph/0110143](#) (2002).
- [3] B. J. Brown, D. Loss, J. K. Pachos, C. N. Self, and J. R. Wootton, Quantum memories at finite temperature, [Reviews of Modern Physics](#) **88**, 045005, [arXiv:1411.6643](#) (2016).
- [4] B. M. Terhal, Quantum error correction for quantum memories, [Reviews of Modern Physics](#) **87**, 307, [arXiv:1302.3428](#) (2015).
- [5] K. Laubscher, D. Loss, and J. R. Wootton, Universal quantum computation in the surface code using non-Abelian islands, [Physical Review A](#) **100**, 012338, [arXiv:1811.06738](#) (2019).
- [6] H. Bombin and M. Martin-Delgado, Quantum Measurements and Gates by Code Deformation, [Journal of Physics A: Mathematical and Theoretical](#) **42**, 095302, [arXiv:0704.2540](#) (2009).
- [7] H. Bombin, Topological order with a twist: Ising anyons from an Abelian model, [Physical Review Letters](#) **105**, 030403, [arXiv:1004.1838](#) (2010).
- [8] B. Yoshida, Topological color code and symmetry-protected topological phases, [Physical Review B](#) **91**, 245131, [arXiv:1503.07208](#) (2015).
- [9] B. J. Brown, K. Laubscher, M. S. Kesselring, and J. R. Wootton, Poking Holes and Cutting Corners to Achieve Clifford Gates with the Surface Code, [Physical Review X](#) **7**, 021029, [arXiv:1609.04673](#) (2017).
- [10] I. Cong, M. Cheng, and Z. Wang, Topological Quantum Computation with Gapped Boundaries, [arXiv:1609.02037](#) (2016).
- [11] I. Cong, M. Cheng, and Z. Wang, Universal Quantum Computation with Gapped Boundaries, [Physical Review Letters](#) **119**, 170504, [arXiv:1707.05490](#) (2017).
- [12] B. Yoshida, Gapped boundaries, group cohomology and fault-tolerant logical gates, [Annals of Physics](#) **377**, 387, [arXiv:1509.03626](#) (2017).
- [13] J. C. Bridgeman, A. C. Doherty, and S. D. Bartlett, Tensor networks with a twist: Anyon-permuting domain walls and defects in projected entangled pair states, [Physical Review B](#) **96**, 245122, [arXiv:1708.08930](#) (2017).
- [14] M. S. Kesselring, F. Pastawski, J. Eisert, and B. J. Brown, The boundaries and twist defects of the color code and their applications to topological quantum computation, [Quantum](#) **2**, 101, [arXiv:1806.02820](#) (2018).

- [15] B. J. Brown, [A fault-tolerant non-Clifford gate for the surface code in two dimensions](#), [arXiv:1903.11634](#) (2020).
- [16] D. Aasen, M. Hell, R. V. Mishmash, A. Higginbotham, J. Danon, M. Leijnse, T. S. Jespersen, J. A. Folk, C. M. Marcus, K. Flensberg, and J. Alicea, Milestones toward majorana-based quantum computing, [Physical Review X](#) **6**, 031016, [arXiv:1511.05153](#) (2015).
- [17] M. Barkeshli, C.-M. Jian, and X.-L. Qi, Theory of defects in Abelian topological states, [Physical Review B](#) **88**, 235103, [arXiv:1305.7203](#) (2013).
- [18] M. Barkeshli, P. Bonderson, M. Cheng, and Z. Wang, Symmetry Fractionalization, Defects, and Gauging of Topological Phases, [Physical Review B](#) **100**, 115147, [arXiv:1410.4540](#) (2019).
- [19] C. Delaney and Z. Wang, Symmetry defects and their application to topological quantum computing, Proceedings of the 2016 AMS Special Session on Topological Phases of Matter and Quantum Computation, [arXiv:1811.02143](#) (2018).
- [20] R. Dijkgraaf and E. Witten, Topological gauge theories and group cohomology, [Communications in Mathematical Physics](#) **129**, 393 (1990).
- [21] G. K. Brennen, M. Aguado, and J. I. Cirac, Simulations of quantum double models, [New Journal of Physics](#) **11**, 053009, [arXiv:0901.1345](#) (2014).
- [22] S. Beigi, P. W. Shor, and D. Whalen, The quantum double model with boundary: Condensations and symmetries, [Communications in Mathematical Physics](#) **306**, 663, [arXiv:1006.5479](#) (2011).
- [23] S. X. Cui, S.-M. Hong, and Z. Wang, Universal quantum computation with weakly integral anyons, [Quantum Information Processing](#) **14**, 26872727, [arXiv:1401.7096](#) (2014).
- [24] I. Cong, M. Cheng, and Z. Wang, Defects between gapped boundaries in two-dimensional topological phases of matter, [Physical Review B](#) **96**, 195129, [arXiv:1703.03564](#) (2017).
- [25] N. Bultinck, M. Mariën, D. Williamson, M. B. Şahinoğlu, J. Haegeman, and F. Verstraete, Anyons and matrix product operator algebras, [Annals of Physics](#) **378**, 183, [arXiv:1511.08090](#) (2017).
- [26] D. J. Williamson, N. Bultinck, and F. Verstraete, Symmetry-enriched topological order in tensor networks: Defects, gauging and anyon condensation, [arXiv:1711.07982](#) (2017).
- [27] C. Shen and L.-Y. Hung, Defect Verlinde Formula for Edge Excitations in Topological Order, [Physical Review Letters](#) **123**, 051602, [arXiv:1901.08285](#) (2019).
- [28] C. Nayak, S. H. Simon, A. Stern, M. Freedman, and S. D. Sarma, Non-abelian anyons and topological quantum computation, [Reviews of Modern Physics](#) **80**, 1083, [arXiv:0707.1889](#) (2007).
- [29] G. Moore and N. Read, Nonabelions in the fractional quantum hall effect, [Nuclear Physics B](#) **360**, 362 (1991).
- [30] A. Stern, Non-Abelian states of matter, [Nature](#) **464**, 187 (2010).
- [31] J. M. Chow, J. M. Gambetta, E. Magesan, D. W. Abraham, A. W. Cross, B. Johnson, N. A. Masluk, C. A. Ryan, J. A. Smolin, S. J. Srinivasan, *et al.*, Implementing a strand of a scalable fault-tolerant quantum computing fabric, [Nature Communications](#) **5**, 4015, [arXiv:1311.6330](#) (2014).
- [32] J. M. Gambetta, J. M. Chow, and M. Steffen, Building logical qubits in a superconducting quantum computing system, [npj Quantum Information](#) **3**, 2, [arXiv:1510.04375](#) (2017).
- [33] M. Levin and X.-G. Wen, String-net condensation: A physical mechanism for topological phases, [Physical Review B](#) **71**, 045110, [arXiv:cond-mat/0404617](#) (2005).
- [34] D. Barter, J. C. Bridgeman, and C. Jones, Domain walls in topological phases and the Brauer-Picard ring for $\text{Vec}(\mathbb{Z}/p\mathbb{Z})$, [Communications in Mathematical Physics](#) **369**, 1167, [arXiv:1806.01279](#) (2019).
- [35] J. C. Bridgeman, D. Barter, and C. Jones, Fusing binary interface defects in topological phases: The $\text{Vec}(\mathbb{Z}/p\mathbb{Z})$ case, [Journal of Mathematical Physics](#) **60**, 121701, [arXiv:1810.09469](#) (2019).
- [36] J. C. Bridgeman and D. Barter, Computing defects associated to bounded domain wall structures: The $\text{Vec}(\mathbb{Z}/p\mathbb{Z})$ case, [Journal of Physics A: Mathematical and Theoretical](#) **10.1088/1751-8121/ab7d60**, in press, [arXiv:1901.08069](#) (2020).
- [37] D. Barter, J. C. Bridgeman, and C. Jones, In preparation.
- [38] P. Etingof, D. Nikshych, and V. Ostrik, Fusion categories and homotopy theory, [Quantum Topology](#) **1**, 209, with an appendix by Ehud Meir, [arXiv:0909.3140](#) (2010).
- [39] P. Etingof, S. Gelaki, D. Nikshych, and V. Ostrik, [Tensor categories](#), Mathematical Surveys and Monographs, Vol. 205 (American Mathematical Society, Providence, RI, 2015) pp. xvi+343.
- [40] D. Tambara and S. Yamagami, Tensor categories with fusion rules of self-duality for finite abelian groups, [Journal of Algebra](#) **209**, 692 (1998).
- [41] S. Gelaki, D. Naidu, and D. Nikshych, Centers of graded fusion categories, [Algebra and Number Theory](#) **3**, 959, [arXiv:0905.3117](#) (2009).
- [42] M. Bischoff, Conformal Net Realizability of Tambara-Yamagami Categories and Generalized Metaplectic Modular Categories, [arXiv:1803.04949](#) (2018).

- [43] Ancillary material can be found at <https://arxiv.org/src/1907.06692/anc>.
- [44] R. Penrose, in *Combinatorial Mathematics and its Applications (Proc. Conf., Oxford, 1969)* (Academic Press, London, 1971) pp. 221–244.
- [45] V. Turaev and A. Virelizier, *Monoidal categories and topological field theory*, Progress in Mathematics, Vol. 322 (Birkhäuser/Springer, Cham, 2017) pp. xii+523.
- [46] J. Fuchs, I. Runkel, and C. Schweigert, TFT construction of RCFT correlators I: partition functions, *Nuclear Physics B* **646**, 353 , [arXiv:hep-th/0204148](https://arxiv.org/abs/hep-th/0204148) (2002).
- [47] A. Kitaev and L. Kong, Models for gapped boundaries and domain walls, *Communications in Mathematical Physics* **313**, 351, [arXiv:1104.5047](https://arxiv.org/abs/1104.5047) (2012).
- [48] J. Fuchs, J. Priel, C. Schweigert, and A. Valentino, On the Brauer groups of symmetries of abelian Dijkgraaf-Witten theories, *Communications in Mathematical Physics* **339**, 385, [arXiv:1404.6646](https://arxiv.org/abs/1404.6646) (2015).
- [49] N. Carqueville, Lecture notes on 2-dimensional defect TQFT, [arXiv:1607.05747](https://arxiv.org/abs/1607.05747) (2016).
- [50] S. Morrison and K. Walker, Blob homology, *Geometry & Topology* **16**, 1481, [arXiv:1009.5025](https://arxiv.org/abs/1009.5025) (2012).
- [51] T. L. (<https://mathoverflow.net/users/360/tyler-lawson>), [Computing an explicit homotopy inverse for \$B\(*, H, *\) \hookrightarrow B\(*, G, G/H\)\$](https://mathoverflow.net/q/288304) , MathOverflow, <https://mathoverflow.net/q/288304> (version: 2017-12-12) (2017).
- [52] A. Ocneanu, Chirality for operator algebras, (*Kyuzeso*, 1993) **39** (1993).
- [53] H. Bombin and M. Martin-Delgado, Topological Quantum Distillation, *Physical Review Letters* **97**, 180501, [arXiv:quant-ph/0605138](https://arxiv.org/abs/quant-ph/0605138) (2006).
- [54] S. Morrison, E. Peters, and N. Snyder, Categories generated by a trivalent vertex, *Selecta Mathematica* **23**, 817, [arXiv:1501.06869](https://arxiv.org/abs/1501.06869) (2017).

A Skein vectors, annular categories and local relations

In this appendix, we define a $(2 + \epsilon)$ -dimensional defect TQFT, Z , which encodes the renormalization invariant properties of all long range entangled, doubled 2D topological phases and their defects. This TQFT first appeared in Ref. [50], but in a somewhat disguised form. A more detailed construction which works in all dimensions is going to appear in the forthcoming paper *Algebraic completions of higher categories* by Morrison and Walker. It is a $(2 + \epsilon)$ theory because we explain how to evaluate path integrals on cylinders, but not all 3-manifolds. As explained by Morrison and Walker in Ref. [50], for a topological theory, path integrals on a cylinder are equivalent to local relations. We have two classes of local relations: those which are required to define $Z(\Sigma)$ where Σ is a domain wall structure or compound defect, and renormalization. Renormalization can modify Σ , which is why we treat it separately.

Definition 17 (Domain wall structure). Let Σ be an oriented surface (possibly with boundary) and $D \subseteq \Sigma$ an embedded 1-dimensional oriented manifold (possibly with boundary) transverse to the boundary of Σ with $\partial D \subseteq \partial \Sigma$. Since D is a manifold, it is diffeomorphic to a disjoint union of oriented circles and oriented intervals connecting boundary components of Σ . In particular, there is no neighborhood of D which is homeomorphic to a trivalent vertex. Label the connected components of $\Sigma \setminus D$ with fusion categories. Let D' be a connected component of D . Since D' and Σ are oriented, we can unambiguously define the left face of D' and the right face of D' . If we let e_2 be a tangent vector which agrees with the orientation of D' , and e_1, e_2 agrees with the orientation of Σ , then e_1 points towards the right face. Let \mathcal{C}_L and \mathcal{C}_R be the fusion categories labeling the left and right faces of D' respectively. We label D' with a bimodule category $\mathcal{C}_L \curvearrowright \mathcal{M} \curvearrowright \mathcal{C}_R$. The pair $D \subseteq \Sigma$ equipped with fusion category and bimodule labels is called a *domain wall structure*.

Definition 18 (Skein vector). Let $D \subseteq \Sigma$ be a domain wall structure. A *skein vector* consists of the following data:

graph: A graph $\Gamma \subseteq \Sigma$ transverse to the boundary of Σ . Edges of Γ are allowed to terminate on the boundary of Σ . Edges of Γ are allowed to terminate on D , but they aren't allowed to cross D . Let $E(\Gamma)$ be the set of edges in Γ and $E(D)$ be the set of edges of D .

edge orientations: An orientation for each edge in $E(\Gamma)$. The edges in $E(D)$ already have a fixed orientation induced from D .

edge labels: Each edge $e \in E(\Gamma)$ lives in a connected component of $\Sigma \setminus D$ which has an associated fusion category \mathcal{C} . We label e with a simple object $l(e)$ in \mathcal{C} . Each edge $f \in E(D)$ has an associated bimodule \mathcal{M} . We label f with a simple object $l(f)$ in \mathcal{M} .

dots: Let v be a vertex internal to $\Sigma \setminus D$. A distinguished base point for E_v , the set of edges adjacent to the vertex v , which we call a *dot*. The orientation of Σ induces a cyclic ordering on E_v , so the base point gives us a linear ordering of E_v , say e_1, \dots, e_d , where e_1 is the distinguished edge. Define $a_i = l(e_i)$. We denote this base point using a dot in one of the sectors around v . The distinguished edge is the first edge encountered starting from the dot following the orientation of the surface:



Vertices which live on D are not given dots. Intuitively, this is because the rotational symmetry is already broken by the orientation of D . The dot method for breaking rotational symmetry is borrowed from Ref. [54].

vertex vectors: Let $v \in \Sigma \setminus D$ be a vertex of Γ in a component with fusion category label \mathcal{C} . Let e_1, \dots, e_d be the adjacent edges starting with the distinguished one. Define

$$o_v(e) = \begin{cases} 1 & e \text{ is pointing towards } v \\ * & e \text{ is oriented away from } v. \end{cases} \quad (59)$$

We label v with a morphism

$$l(e_1)^{o_v(e_1)} l(e_2)^{o_v(e_2)} \dots l(e_d)^{o_v(e_d)} \rightarrow 1 \quad (60)$$

in \mathcal{C} . For example, the vertex in Eqn. 58 is labeled with a morphism $a_1^* a_2 a_3^* a_4^* a_5 \rightarrow 1$. There are four types of vertices which live on D . If M is the bimodule which labels the relevant component of D , the vertices are labeled with morphisms in \mathcal{M} as follows:

$$\begin{array}{ccc} \begin{array}{c} n \\ \text{---} \uparrow \text{---} \\ a \rightarrow \text{---} \uparrow \text{---} \\ m \end{array} & : am \rightarrow n & \begin{array}{c} n \\ \text{---} \uparrow \text{---} \\ a \leftarrow \text{---} \uparrow \text{---} \\ m \end{array} : a^* m \rightarrow n \end{array} \quad (61a)$$

$$\begin{array}{ccc} \begin{array}{c} n \\ \text{---} \uparrow \text{---} \\ \text{---} \leftarrow b \\ m \end{array} & : mb \rightarrow n & \begin{array}{c} n \\ \text{---} \uparrow \text{---} \\ \text{---} \rightarrow b \\ m \end{array} : mb^* \rightarrow n \end{array} \quad (61b)$$

For computational reasons, we require each vertex in Γ to have valence 3. This is general since higher valence vertices can always be decomposed into trivalent vertices.

Definition 19 (Skein local relations). If $D \subseteq \Sigma$ is a domain wall structure, we define

$$Z(\Sigma) = \mathbb{C}\{\text{skein vectors on } D \subseteq \Sigma\} / \text{local relations}. \quad (62)$$

We have the following local relations:

isotopy: We can isotope Γ inside Σ .

orientation: We can reverse the orientation on an edge in $\Sigma \setminus D$ and take the dual of the corresponding label.

dot: Moving the dot one sector following the orientation of Σ corresponds to transforming the vertex vector using the rigid structure:

$$\begin{array}{ccc} \begin{array}{c} a_3 \\ \text{---} \nearrow \text{---} \\ a_1 \rightarrow \text{---} \uparrow \text{---} \\ a_2 \end{array} & \rightarrow & \begin{array}{c} a_3 \\ \text{---} \nearrow \text{---} \\ a_1 \rightarrow \text{---} \downarrow \text{---} \\ a_2 \end{array} \end{array} \quad (63a)$$

$$\begin{array}{ccc} \begin{array}{c} \text{---} \nearrow \text{---} \\ a_1 \quad a_2 \quad a_3 \end{array} & \rightarrow & \begin{array}{c} \text{---} \nearrow \text{---} \\ a_2 \quad a_3 \quad a_1 \end{array} \end{array} \quad (63b)$$

$$\mathbf{F} : \begin{array}{c} d \\ \text{---} \uparrow \text{---} \\ \bullet \quad \beta \\ \text{---} \nearrow \text{---} \quad \text{---} \searrow \text{---} \\ \bullet \quad \alpha \quad e \\ \text{---} \nearrow \text{---} \quad \text{---} \searrow \text{---} \\ a \quad b \quad c \end{array} = \sum_{\mu\nu} F_{\alpha\beta}^{\mu\nu} \begin{array}{c} d \\ \text{---} \uparrow \text{---} \\ \bullet \quad \nu \\ \text{---} \nearrow \text{---} \quad \text{---} \searrow \text{---} \\ \bullet \quad f \quad \mu \\ \text{---} \nearrow \text{---} \quad \text{---} \searrow \text{---} \\ a \quad b \quad c \end{array} \quad (63c)$$

$$\mathbf{G} : \quad \begin{array}{c} a \\ \bullet \\ \beta \\ \text{---} \\ b \quad c \\ \alpha \\ \bullet \\ a \end{array} = G_{\alpha\beta} \quad \begin{array}{c} a \\ \text{---} \\ a \end{array} \quad (63d)$$

$$\mathbf{L} : \quad \begin{array}{c} n \\ \zeta \\ \text{---} \\ a \\ \eta \\ \text{---} \\ b \\ m \end{array} = \sum_{\alpha\mu} L_{\eta\zeta}^{\alpha\mu} \quad \begin{array}{c} n \\ \text{---} \\ a \quad c \\ \alpha \\ \text{---} \\ b \quad \mu \\ m \end{array} \quad (63e)$$

$$\mathbf{R} : \quad \begin{array}{c} n \\ \zeta \\ \text{---} \\ a \\ \eta \\ \text{---} \\ b \\ m \end{array} = \sum_{\alpha\mu} R_{\eta\zeta}^{\alpha\mu} \quad \begin{array}{c} n \\ \text{---} \\ \mu \quad c \\ \alpha \\ \text{---} \\ a \quad b \\ m \end{array} \quad (63f)$$

$$\mathbf{C} : \quad \begin{array}{c} n \\ \zeta \\ \text{---} \\ b \\ \eta \\ \text{---} \\ a \\ m \end{array} = \sum_{\mu\nu} C_{\eta\zeta}^{\mu\nu} \quad \begin{array}{c} n \\ \text{---} \\ \nu \\ \mu \\ \text{---} \\ a \quad b \\ m \end{array} \quad (63g)$$

$$\mathbf{LG} : \quad \begin{array}{c} n \\ \zeta \\ \text{---} \\ \eta \\ m \end{array} = LG_{\eta\zeta} \quad \begin{array}{c} n \\ \text{---} \\ m \end{array} \quad (63h)$$

$$\mathbf{RG} : \quad \begin{array}{c} n \\ \zeta \\ \text{---} \\ \eta \\ m \end{array} = RG_{\eta\zeta} \quad \begin{array}{c} n \\ \text{---} \\ m \end{array} \quad (63i)$$

From the local relations \mathbf{G}, \mathbf{LG} and \mathbf{RG} respectively, we get:

$$\mathbf{Inverse\ G} : \quad \begin{array}{c} \text{---} \\ a \quad b \end{array} = \sum_{\alpha\beta} G_{\alpha\beta}^{-1} \quad \begin{array}{c} \text{---} \\ \beta \\ \text{---} \\ \alpha \\ \text{---} \\ a \quad b \end{array} \quad (63j)$$

bubble :

$$\begin{array}{|c|} \hline \text{bubble :} \\ \hline \end{array} \quad \begin{array}{c} \text{Diagram: A circle with a clockwise arrow inside, labeled } a. \\ \text{Equation: } = \dim(a) \end{array} \quad \begin{array}{c} \text{Diagram: A dashed square box.} \end{array} \quad (63k)$$

InverseLG :

$$\begin{array}{|c|} \hline \text{InverseLG :} \\ \hline \end{array} \quad \begin{array}{c} \text{Diagram: Two vertical lines, left black labeled } a, \text{ right red labeled } m. \\ \text{Equation: } = \sum_{\zeta\eta} LG_{\zeta\eta}^{-1} \end{array} \quad \begin{array}{c} \text{Diagram: A red line with a black arrow labeled } \eta \text{ and a black arrow labeled } \zeta. \\ \text{Labels: } a, m \end{array} \quad (63l)$$

InverseRG :

$$\begin{array}{|c|} \hline \text{InverseRG :} \\ \hline \end{array} \quad \begin{array}{c} \text{Diagram: Two vertical lines, left red labeled } m, \text{ right black labeled } b. \\ \text{Equation: } = \sum_{\zeta\eta} RG_{\zeta\eta}^{-1} \end{array} \quad \begin{array}{c} \text{Diagram: A red line with a black arrow labeled } \eta \text{ and a black arrow labeled } \zeta. \\ \text{Labels: } m, b \end{array} \quad (63m)$$

Definition 20 (representation theory of categories). Let \mathcal{C} be a category. A *representation* of \mathcal{C} is a functor $V : \mathcal{C} \rightarrow \mathbf{Vec}$ from \mathcal{C} into the category of vector spaces. The functor V consists of a vector space V_a for each object $a \in \mathcal{C}$ and a linear map $V_f : V_a \rightarrow V_b$ for each morphism $f : a \rightarrow b$ in \mathcal{C} such that $V_f \circ V_g = V_{f \circ g}$ and $V_{\text{id}} = \text{id}$.

We are particularly interested in the following computational problem: Let \mathcal{C} be a category. If \mathcal{C} is semi-simple, compute a complete list of simple representations of \mathcal{C} . The first step in computing the representations of \mathcal{C} is computing the Karoubi envelope:

Definition 21 (Karoubi envelope). Let \mathcal{C} be a category. The Karoubi envelope of \mathcal{C} is a category defined as follows: The objects are idempotent endomorphisms in \mathcal{C} . A morphism between two such idempotents $i : a \rightarrow a$ and $j : b \rightarrow b$ is a morphism $f : a \rightarrow b$ such that $jfi = f$. If \mathcal{C} is semi-simple, we can compute the Karoubi envelope of \mathcal{C} as follows:

1. For each object $a \in \mathcal{C}$, compute an *Artin-Wedderburn isomorphism* $\text{End}(a) \cong \prod_{i=1}^d M_i$ where each M_i is a matrix algebra. The idempotents e_{11} from each factor in this product are non isomorphic simple objects in the Karoubi envelope of \mathcal{C} . Computing Artin-Wedderburn decompositions is computationally hard, but possible for algebras of small (< 50) dimension. This is demonstrated in the Mathematica notebook `AWdecomposition.nb` in the ancillary material[43].
2. Given two idempotents i, j , solving the linear equation $jfi = f$ gives the morphisms between i and j .

The Karoubi envelope of \mathcal{C} is equivalent to the category of representations of \mathcal{C} . Given a simple object $i : a \rightarrow a$ in the Karoubi envelope, the corresponding representation is $\mathcal{C}(a, -)i$. Computing bases and action matrices for this representation is a linear algebra problem.

Definition 22 (Annular categories and point defects). Let $D \subseteq \Sigma$ be a domain wall structure. If Σ has a boundary, then $Z(\Sigma)$ has more structure than just a vector space. In a neighborhood of a boundary component, the domain wall structure looks like:

$$\begin{array}{|c|} \hline \text{Diagram: A dashed circle with a central white circle. Three lines enter from the top: a green line with an arrow pointing down, a blue line with an arrow pointing right, and a red line with an arrow pointing down-left.} \\ \hline \end{array} \quad (64)$$

In general, there can be an arbitrary number of components of D terminating on the boundary, but for the sake of clarity, we shall work with this explicit example. In a neighborhood of the boundary component, a skein vector looks like:

$$\begin{array}{|c|} \hline \text{Diagram: A dashed circle with a central white circle. Four lines enter from the top: a green line with an arrow pointing down labeled } z, \text{ a blue line with an arrow pointing right labeled } y, \text{ a red line with an arrow pointing down-left labeled } x, \text{ and a black line with an arrow pointing down-right labeled } w. \\ \hline \end{array} \quad (65)$$

We define a domain wall structure

$$A = \text{Diagram of a disk with a central white circle and three colored rays (green, blue, red) meeting at the center. The green ray points up, the blue ray points right, and the red ray points down-left. The disk has a grey grid background.} \quad (66)$$

Every skein vector on A is equivalent a sum of skein vectors of the following form:

$$\text{Diagram of a disk with a central white circle. A green ray labeled } \beta \text{ points up from the center, labeled } \alpha \text{ near the boundary. A blue ray labeled } \mu \text{ points right from the center, labeled } \nu \text{ near the boundary. A red ray labeled } \eta \text{ points down-left from the center, labeled } \zeta \text{ near the boundary. Black arcs connect the rays. Labels } p, n, m \text{ are near the center. The disk has a grey grid background.} \in Z(A). \quad (67)$$

The space $Z(A)$ forms a category. The objects are tuples of module category objects (x, y, z) and the morphisms are skein vectors Eqn. 67. Composition is given by gluing one skein vector inside the other, subject to matching labels. We call $Z(A)$ an *annular category*. We can glue Eqn. 67 into Eqn. 65. Therefore, $Z(\Sigma)$ has an action of the annular category associated to each boundary component. Suppose that V is a representation of the annular category $Z(A)$. We also call V a *point defect*. Vectors in V are depicted as follows:

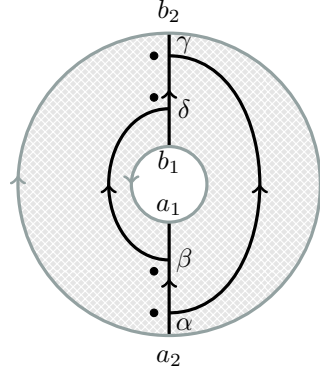
$$\text{Diagram of a disk with a dashed boundary. A green ray labeled } p \text{ points up from the center, labeled } v \text{ near the center. A blue ray labeled } n \text{ points right from the center. A red ray labeled } m \text{ points down-left from the center. The disk has a grey grid background.} \in V_{m,n,p}. \quad (68)$$

Diagrammatically, the annular category action of Eqn. 67 on Eqn. 68 looks like:

$$\text{Diagram of a disk with a dashed boundary, containing the skein vector from Eqn. 67, with labels } x, y, z \text{ at the boundary.} = \sum_w A_{\eta\zeta\mu\nu\alpha\beta v}^w \text{Diagram of a disk with a dashed boundary, containing the point defect from Eqn. 68, with labels } x, y, z \text{ at the boundary.} \quad (69)$$

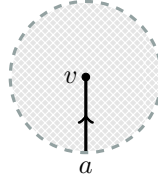
For the special case in Example 23, the annular category coincides with the tube algebra[25, 26, 52].

Example 23 (Anyons). Consider the following annular category for a fusion category \mathcal{C} :



$$: (a_1, b_1) \rightarrow (a_2, b_2) \quad (70)$$

Representations V of this annular category parameterize anyons in the Levin-Wen phase associated to \mathcal{C} . Vectors



$$\in V_{(a,1)} \quad (71)$$

are important because they can terminate a fusion category string in a compound defect skein vector (defined below).

Definition 24 (Compound defect). A *compound defect* consists of a domain wall structure $D \subseteq \Sigma$ and an annular category representation for each boundary component of Σ .

Definition 25 (Compound defect skein vector). Let $D \subseteq \Sigma$ be a compound defect. A compound defect skein vector consists of a skein vector for the domain wall structure and a vector in each boundary component representation. We require the object labels on the vector and the boundary component to match.

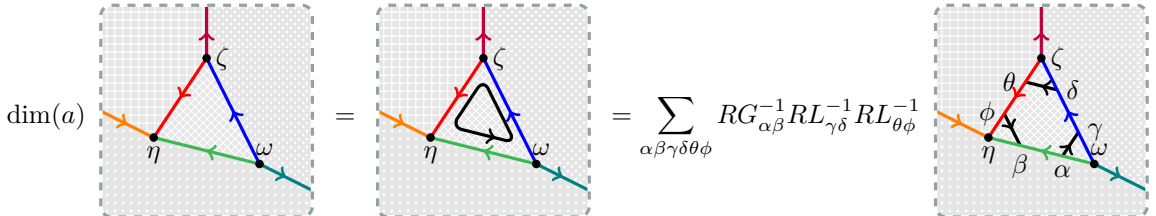
Definition 26 (Local relations). Let Σ be a compound defect. Again, we define

$$Z(\Sigma) = \mathbb{C}\{\text{skein vectors}\} / \text{local relations}. \quad (72)$$

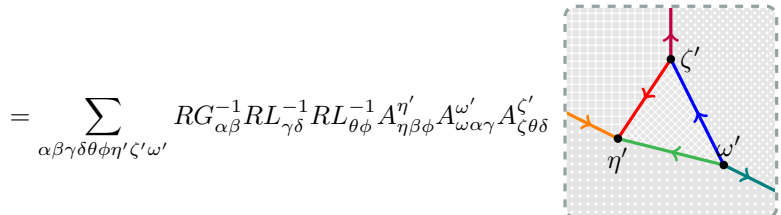
We have all the local relations from Definition 19. There is one additional local relation:

annular category action: A vector which was used to fill a boundary component of Σ can absorb a skein vector on the surrounding annulus and transform according to its annular category representation. This is depicted in Eqn. 69.

An important consequence of the annular category action local relation is the bubble action local relation:



$$\dim(a) \quad (73)$$



$$= \sum_{\alpha\beta\gamma\delta\phi\eta'\zeta'\omega'} RG_{\alpha\beta}^{-1} RL_{\gamma\delta}^{-1} RL_{\theta\phi}^{-1} A_{\eta\beta\phi}^{\eta'} A_{\omega\alpha\gamma}^{\omega'} A_{\zeta\theta\delta}^{\zeta'} \quad (74)$$

This local relation is closely related to the bubble term in the Levin-Wen Hamiltonian from Ref. [33]. We have

$$\begin{aligned}
 & \text{Diagram (75)} = \frac{1}{\dim(\mathcal{C})} \sum_a \dim(a)^2 \text{Diagram (75)} \\
 & \text{Diagram (76)} = \frac{1}{\dim(\mathcal{C})} \sum_a \dim(a) \text{Diagram (76)}
 \end{aligned} \tag{75}$$

$$\text{Diagram (76)} = \frac{1}{\dim(\mathcal{C})} \sum_a \dim(a) \text{Diagram (76)} \tag{76}$$

Definition 27 (renormalization). All the local relations described above apply to a fixed domain wall structure and are sufficient to construct $Z(\Sigma)$. Now we describe a procedure which can modify the compound defect Σ , which we call *renormalization*. Choose an open ball in Σ . For example it might look like:

$$C = \text{Diagram (77)} \tag{77}$$

The vector space $Z(C)$ forms a representation W of the boundary annular category. Define

$$C' = \text{Diagram (78)} \tag{78}$$

Renormalization modifies Σ by replacing C with C' and applies the annular category intertwining isomorphism $Z(C) \rightarrow Z(C')$ to the skein vectors on C . This is the justification for calling annular categories “*local observable algebras*”. If there is an isomorphism of annular category representations which sends one skein vector to another, then they are equivalent up to renormalization.

Example 28 (Anyon braidings). Let V be a representation of the annular category from Example 23. The central idempotents in an annular category measure anyon charge. We have the following isomorphism of annular category

representations because the left and right sides both have charge V :

$$(79)$$

Applied to the vector in Eqn. 71, the isomorphism has the following form:

$$(80)$$

Notice that the internal state of the anyon can change as it passes through the a string.

Definition 29 (Ladder category). Consider the following domain wall structure:

$$(81)$$

The skein vectors in $Z(L)$ assemble into a category. The objects are pairs of objects $(m \in \mathcal{M}, n \in \mathcal{N})$. The morphisms are skein vectors of the following form:

$$(82)$$

Composition is given by vertical gluing of the skein vectors and then reducing back to the form in Eqn. 82 using local relations. The Karoubi envelope of $Z(L)$ is equivalent to the bimodule category $\mathcal{M} \otimes_{\mathcal{B}} \mathcal{N}$. As explained in Definition 21, objects in the Karoubi envelope are idempotents

$$(83)$$

Left trivalent vertices in the Karoubi envelope are skein vectors

$$(84)$$

which absorb the idempotent j on the top and the idempotent

$$\sum_{\zeta\eta} i_{\zeta\eta} \quad \begin{array}{c} \text{---} m \quad n \text{---} \\ \text{---} a \quad m \quad n \text{---} \end{array} \quad (85)$$

on the bottom. Right vertices are defined analogously. Computing these Karoubi envelope trivalent vertices is a linear algebra problem, and the solutions form a vector space. If we also require that the vertices Eqn. 84 have left, center and right associators matching bimodules from our original list, then we cut the solution space down to a finite set, which may have more than one element. When we talk about vertices in the Karoubi envelope of a ladder category, we will always assume that they have been chosen to have associators matching our original models. Computing a complete set of trivalent vertices in the Karoubi envelope of the ladder category gives us the decompositions $\mathcal{M} \otimes_{\mathcal{B}} \mathcal{N} \cong \oplus_i \mathcal{P}_i$ which are tabulated in the Brauer-Picard tables.

Definition 30 (Inflation trick). We are interested in computing explicit representations of annular categories with three bimodule strings. This is a computationally hard problem even for annular categories with two bimodule strings. Moreover, we have isomorphisms

$$\begin{array}{c} \text{---} A_2 \text{---} \\ \text{---} A_1 \text{---} \end{array} \quad \begin{array}{c} \text{---} A_3 \text{---} \\ \text{---} V \text{---} \end{array} \quad \cong \quad \begin{array}{c} \text{---} W \text{---} \end{array} \quad (86)$$

which gives us an equivalence relation on three bimodule string annular category representations. The *inflation trick* produces one representation from each equivalence class without needing to compute the representation theory of algebras with large dimension. It works as follows: If $\mathcal{A} \curvearrowright \mathcal{M} \curvearrowright \mathcal{B}$ is a bimodule, then defects interfacing between \mathcal{M} and itself form a (multi) fusion category $\text{End}(\mathcal{M})$:

$$\begin{array}{c} V_1 \\ V_2 \end{array} \quad \cong \quad \bigoplus_i \quad \begin{array}{c} W_i \end{array} \quad (87)$$

If \mathcal{M} is indecomposable, then $\text{End}(\mathcal{M})$ is a fusion category Morita equivalent to $\mathcal{A} \otimes \mathcal{B}^{\text{rev}}$. In particular, $\text{End}(\mathcal{M})$ has a unit object, represented as an idempotent:

$$\sum_{\zeta\eta\theta\phi} E_{\zeta\eta\theta\phi} \quad \begin{array}{c} n \\ \phi \\ \theta \\ n \\ m \\ \eta \\ \zeta \\ m \end{array} \quad (88)$$

If we replace the trivalent vertices on the top (bottom) half of the idempotent with trivalent vertices in the Karoubi envelope of a ladder category corresponding to an embedding $\mathcal{M} \hookrightarrow \mathcal{P} \otimes_{\mathcal{B}} \mathcal{Q}$, then we get an idempotent in a 3 bimodule string annular category which encodes the functor $\mathcal{M} \hookrightarrow \mathcal{P} \otimes_{\mathcal{B}} \mathcal{Q}$.

Definition 31 (Associators for vertical defect fusion). We shall denote annular category intertwining maps

$$\Theta : \begin{array}{|c|} \hline V_1 \\ \hline V_2 \\ \hline \end{array} \rightarrow \begin{array}{|c|} \hline W \\ \hline \end{array} \quad (89)$$

using squiggly trivalent vertices:

$$\begin{array}{|c|} \hline V_1 \\ \hline V_2 \\ \hline \end{array} \xrightarrow{\Theta} \begin{array}{|c|} \hline W \\ \hline \end{array} \quad (90)$$

The squiggly lines represent a renormalization process. The change of basis matrix $F_{\Theta\Phi}^{\Xi\Psi}$ between the following intertwining maps

$$\begin{array}{|c|} \hline V_1 \\ \hline V_2 \\ \hline V_3 \\ \hline \end{array} \xrightarrow{\Theta} \begin{array}{|c|} \hline X_1 \\ \hline X_2 \\ \hline \end{array} \xrightarrow{\Phi} \begin{array}{|c|} \hline W \\ \hline \end{array} \quad (91a)$$

$$\begin{array}{|c|} \hline V_1 \\ \hline V_2 \\ \hline V_3 \\ \hline \end{array} \xrightarrow{\Xi} \begin{array}{|c|} \hline Y_1 \\ \hline Y_2 \\ \hline \end{array} \xrightarrow{\Psi} \begin{array}{|c|} \hline W \\ \hline \end{array} \quad (91b)$$

is the associator for vertical defect fusion. This allows us to compute the associator for $\text{End}(\mathcal{M})$.

B Domain wall definitions

Name	Subgroup $\leq S_3$	# inequiv. cocycles	Cocycle formula
\mathcal{A}_1	$\{0\}$	1	+1
\mathcal{A}_2	$\mathbb{Z}/3\mathbb{Z} \cong \langle(0, 1)\rangle$	1	+1
\mathcal{A}_3	$\mathbb{Z}/2\mathbb{Z} \cong \langle(1, 0)\rangle$	1	+1
\mathcal{A}_4	$S_3 \cong \langle(1, 0), (0, 1)\rangle$	1	+1

Table 2: Defining data for $\mathbf{Vec}|\mathbf{Vec}(S_3)$ bimodules. Names \mathcal{A}_i consistent with Ref. [24]

Name	Subgroup $\leq \mathbb{Z}/2\mathbb{Z} \times S_3$	# inequiv. cocycles	Cocycle formula
K_1	$\{0\}$	1	+1
K_2	$\mathbb{Z}/2\mathbb{Z} \cong \langle(0, 1, 0)\rangle$	1	+1
K_3	$\mathbb{Z}/2\mathbb{Z} \cong \langle(1, 0, 0)\rangle$	1	+1
K_4	$\mathbb{Z}/2\mathbb{Z} \cong \langle(1, 1, 0)\rangle$	1	+1
K_5	$\mathbb{Z}/3\mathbb{Z} \cong \langle(0, 0, 1)\rangle$	1	+1
$K_{6,p}$	$\mathbb{Z}/2\mathbb{Z} \times \mathbb{Z}/2\mathbb{Z} \cong \langle(1, 0, 0), (0, 1, 0)\rangle$	2	$\Omega_p(g, h) = (-1)^{pg_1h_2}$
K_7	$\mathbb{Z}/6\mathbb{Z} \cong \langle(1, 0, 1)\rangle$	1	+1
K_8	$S_3 \cong \langle(0, 1, 0), (0, 0, 1)\rangle$	1	+1
K_9	$S_3 \cong \langle(1, 1, 0), (0, 0, 1)\rangle$	1	+1
$K_{10,p}$	$\mathbb{Z}/2\mathbb{Z} \times S_3 \cong \langle(1, 0, 0), (0, 1, 0), (0, 0, 1)\rangle$	2	$\Omega_p(g, h) = (-1)^{pg_1h_2}$

Table 3: Defining data for $\mathbf{Vec}(\mathbb{Z}/2\mathbb{Z})|\mathbf{Vec}(S_3)$ bimodules. Names K_i consistent with Ref. [5], with the left and right versions of each domain wall given the same name.

Name	Subgroup $\leq \mathbb{Z}/3\mathbb{Z} \times S_3$	# inequiv. cocycles	Cocycle formula
Q_1	$\{0\}$	1	+1
Q_2	$\mathbb{Z}/2\mathbb{Z} \cong \langle(0, 1, 0)\rangle$	1	+1
Q_3	$\mathbb{Z}/3\mathbb{Z} \cong \langle(0, 0, 1)\rangle$	1	+1
Q_4	$\mathbb{Z}/3\mathbb{Z} \cong \langle(1, 0, 0)\rangle$	1	+1
Q_8	$\mathbb{Z}/3\mathbb{Z} \cong \langle(1, 0, 1)\rangle$	1	+1
Q_5	$S_3 \cong \langle(0, 1, 0), (0, 0, 1)\rangle$	1	+1
Q_6	$\mathbb{Z}/6\mathbb{Z} \cong \langle(1, 1, 0)\rangle$	1	+1
$Q_{9,p}$	$\mathbb{Z}/3\mathbb{Z} \times \mathbb{Z}/3\mathbb{Z} \cong \langle(1, 0, 0), (0, 0, 1)\rangle$	2	$\Omega_p(g, h) = \omega^{pg_1h_3}$
Q_7	$\mathbb{Z}/\mathbb{Z}3 \times S_3 \cong \langle(1, 0, 1), (0, 1, 0)\rangle$	1	+1

Table 4: Defining data for $\mathbf{Vec}(\mathbf{Vec}(\mathbb{Z}/3\mathbb{Z}))|\mathbf{Vec}(S_3)$ bimodules. Names Q_i chosen such that the left and right versions of each bimodule given the same name.

Name	Subgroup $\leq S_3 \times S_3$	# inequiv. cocycles	Cocycle formula
T	$\{0\}$	1	+1
R_2	$\mathbb{Z}/2\mathbb{Z} \cong \langle (0, 0, 1, 0) \rangle$	1	+1
L_2	$\mathbb{Z}/2\mathbb{Z} \cong \langle (1, 0, 0, 0) \rangle$	1	+1
I_2	$\mathbb{Z}/2\mathbb{Z} \cong \langle (1, 0, 1, 0) \rangle$	1	+1
R_3	$\mathbb{Z}/3\mathbb{Z} \cong \langle (0, 0, 0, 1) \rangle$	1	+1
L_3	$\mathbb{Z}/3\mathbb{Z} \cong \langle (0, 1, 0, 0) \rangle$	1	+1
I_3	$\mathbb{Z}/3\mathbb{Z} \cong \langle (0, 1, 0, 1) \rangle$	1	+1
$A_{2,p}$	$\mathbb{Z}/2\mathbb{Z} \times \mathbb{Z}/2\mathbb{Z} \cong \langle (1, 0, 0, 0), (0, 0, 1, 0) \rangle$	2	$\Omega_p(g, h) = (-1)^{pg_1h_3}$
R	$S_3 \cong \langle (0, 0, 1, 0), (0, 0, 0, 1) \rangle$	1	+1
L	$S_3 \cong \langle (1, 0, 0, 0), (0, 1, 0, 0) \rangle$	1	+1
I	$S_3 \cong \langle (1, 0, 1, 0), (0, 1, 0, 1) \rangle$	1	+1
C_R	$S_3 \cong \langle (1, 0, 1, 0), (0, 0, 0, 1) \rangle$	1	+1
C_L	$S_3 \cong \langle (1, 0, 1, 0), (0, 1, 0, 0) \rangle$	1	+1
B_{23}	$\mathbb{Z}/6\mathbb{Z} \cong \langle (1, 0, 0, 0), (0, 0, 0, 1) \rangle$	1	+1
B_{32}	$\mathbb{Z}/6\mathbb{Z} \cong \langle (0, 1, 0, 0), (0, 0, 1, 0) \rangle$	1	+1
$A_{3,p}$	$\mathbb{Z}/3\mathbb{Z} \times \mathbb{Z}/3\mathbb{Z} \cong \langle (0, 1, 0, 0), (0, 0, 0, 1) \rangle$	2	$\Omega_p(g, h) = \omega^{pg_2h_4}$
$D_{R,p}$	$S_3 \times \mathbb{Z}/2\mathbb{Z} \cong \langle (1, 0, 0, 0), (0, 0, 1, 0), (0, 0, 0, 1) \rangle$	2	$\Omega_p(g, h) = (-1)^{pg_1h_3}$
$D_{L,p}$	$S_3 \times \mathbb{Z}/2\mathbb{Z} \cong \langle (1, 0, 0, 0), (0, 1, 0, 0), (0, 0, 1, 0) \rangle$	2	$\Omega_p(g, h) = (-1)^{pg_1h_3}$
E_R	$S_3 \times \mathbb{Z}/3\mathbb{Z} \cong \langle (0, 1, 0, 0), (0, 0, 1, 0), (0, 0, 0, 1) \rangle$	1	+1
E_L	$S_3 \times \mathbb{Z}/3\mathbb{Z} \cong \langle (1, 0, 0, 0), (0, 1, 0, 0), (0, 0, 0, 1) \rangle$	1	+1
G_p	$(\mathbb{Z}/3\mathbb{Z} \times \mathbb{Z}/3\mathbb{Z}) \rtimes \mathbb{Z}/2\mathbb{Z} \cong \langle (1, 0, 1, 0), (0, 1, 0, 0), (0, 0, 0, 1) \rangle$	2	$\Omega_p(g, h) = (-1)^{p(1+h_1)g_2h_4}$
F_p	$S_3 \times S_3 \cong \langle (1, 0, 0, 0), (0, 1, 0, 0), (0, 0, 1, 0), (0, 0, 0, 1) \rangle$	2	$\Omega_p(g, h) = (-1)^{pg_1h_3}$

Table 5: Defining data for $\mathbf{Vec}(S_3) | \mathbf{Vec}(S_3)$ bimodules

C Brauer-Picard tables (domain wall fusion)

In this appendix, we provide complete tables of the fusion rules for bimodules between $\mathbf{Vec}(S_3)$ and \mathbf{Vec} , $\mathbf{Vec}(\mathbb{Z}/2\mathbb{Z})$, $\mathbf{Vec}(\mathbb{Z}/3\mathbb{Z})$, and $\mathbf{Vec}(S_3)$.

$\otimes \mathbf{Vec}$	\mathcal{A}_1	\mathcal{A}_2	\mathcal{A}_3	\mathcal{A}_4	$\otimes \mathbf{Vec}(S_3)$	\mathcal{A}_1	\mathcal{A}_2	\mathcal{A}_3	\mathcal{A}_4
\mathcal{A}_1	T	R_3	R_2	R	\mathcal{A}_1	$6T_0$	$2T_0$	$3T_0$	T_0
\mathcal{A}_2	L_3	$A_{3,0}$	B_{32}	E_R	\mathcal{A}_2	$2T_0$	$6T_0$	T_0	$3T_0$
\mathcal{A}_3	L_2	B_{23}	$A_{2,0}$	$D_{R,0}$	\mathcal{A}_3	$3T_0$	T_0	$3T_0$	$2T_0$
\mathcal{A}_4	L	E_L	$D_{L,0}$	F_0	\mathcal{A}_4	T_0	$3T_0$	$2T_0$	$3T_0$

Table 6: Domain wall fusion for $\mathbf{Vec}(S_3)|\mathbf{Vec}$ domain walls with $\mathbf{Vec}|\mathbf{Vec}(S_3)$ domain walls.

Any $\mathbf{Vec}(S_3)$ bimodule \mathcal{B} that occurs in Table 6 is actually the composite of two module categories.

$$\begin{array}{|c|} \hline \mathcal{B} \\ \hline \end{array} \cong \begin{array}{|c|} \hline \mathcal{M} \\ \hline \end{array} \begin{array}{|c|} \hline \mathcal{N} \\ \hline \end{array}. \quad (92)$$

Similar statements can be made for the remaining tables in this appendix. This allows us to identify bimodules that ‘factor through’ a subcategory.

$\otimes \mathbf{Vec}(\mathbb{Z}/2\mathbb{Z})$	K_1	K_2	K_3	K_5	$K_{6,0}$	K_7	K_8	$K_{10,0}$	K_4	$K_{6,1}$	K_9	$K_{10,1}$
K_1	$2T$	$2R_2$	T	$2R_3$	R_2	R_3	$2R$	R	T	R_2	R_3	R
K_2	$2L_2$	$2A_{2,0}$	L_2	$2B_{23}$	$A_{2,0}$	B_{23}	$2D_{R,0}$	$D_{R,0}$	L_2	$A_{2,0}$	B_{23}	$D_{R,0}$
K_3	T	R_2	$2T$	R_3	$2R_2$	$2R_3$	R	$2R$	R_2	T	R	R_3
K_5	$2L_3$	$2B_{32}$	L_3	$2A_{3,0}$	B_{32}	$A_{3,0}$	$2E_R$	E_R	L_3	B_{32}	$A_{3,0}$	E_R
$K_{6,0}$	L_2	$A_{2,0}$	$2L_2$	B_{23}	$2A_{2,0}$	$2B_{23}$	$D_{R,0}$	$2D_{R,0}$	$A_{2,0}$	L_2	$D_{R,0}$	B_{23}
K_7	L_3	B_{32}	$2L_3$	$A_{3,0}$	$2B_{32}$	$2A_{3,0}$	E_R	$2E_R$	B_{32}	L_3	E_R	$A_{3,0}$
K_8	$2L$	$2D_{L,0}$	L	$2E_L$	$D_{L,0}$	E_L	$2F_0$	F_0	L	$D_{L,0}$	E_L	F_0
$K_{10,0}$	L	$D_{L,0}$	$2L$	E_L	$2D_{L,0}$	$2E_L$	F_0	$2F_0$	$D_{L,0}$	L	F_0	E_L
K_4	T	R_2	L_2	R_3	$A_{2,0}$	B_{23}	R	$D_{R,0}$	I_2	$A_{2,1}$	C_R	$D_{R,1}$
$K_{6,1}$	L_2	$A_{2,0}$	T	B_{23}	R_2	R_3	$D_{R,0}$	R	$A_{2,1}$	I_2	$D_{R,1}$	C_R
K_9	L_3	B_{32}	L	$A_{3,0}$	$D_{L,0}$	E_L	E_R	F_0	C_L	$D_{L,1}$	G_0	F_1
$K_{10,1}$	L	$D_{L,0}$	L_3	E_L	B_{32}	$A_{3,0}$	F_0	E_R	$D_{L,1}$	C_L	F_1	G_0

$\otimes \mathbf{Vec}(S_3)$	K_1	K_2	K_3	K_5	$K_{6,0}$	K_7	K_8	$K_{10,0}$	K_4	$K_{6,1}$	K_9	$K_{10,1}$
K_1	$6T^{\mathbb{Z}/2\mathbb{Z}}$	$3T^{\mathbb{Z}/2\mathbb{Z}}$	$6R^{\mathbb{Z}/2\mathbb{Z}}$	$2T^{\mathbb{Z}/2\mathbb{Z}}$	$3R^{\mathbb{Z}/2\mathbb{Z}}$	$2R^{\mathbb{Z}/2\mathbb{Z}}$	$T^{\mathbb{Z}/2\mathbb{Z}}$	$R^{\mathbb{Z}/2\mathbb{Z}}$	$3T^{\mathbb{Z}/2\mathbb{Z}}$	$3R^{\mathbb{Z}/2\mathbb{Z}}$	$T^{\mathbb{Z}/2\mathbb{Z}}$	$R^{\mathbb{Z}/2\mathbb{Z}}$
K_2	$3T^{\mathbb{Z}/2\mathbb{Z}}$	$3T^{\mathbb{Z}/2\mathbb{Z}}$	$3R^{\mathbb{Z}/2\mathbb{Z}}$	$T^{\mathbb{Z}/2\mathbb{Z}}$	$3R^{\mathbb{Z}/2\mathbb{Z}}$	$R^{\mathbb{Z}/2\mathbb{Z}}$	$2T^{\mathbb{Z}/2\mathbb{Z}}$	$2R^{\mathbb{Z}/2\mathbb{Z}}$	$R^{\mathbb{Z}/2\mathbb{Z}} + T^{\mathbb{Z}/2\mathbb{Z}}$	$R^{\mathbb{Z}/2\mathbb{Z}} + T^{\mathbb{Z}/2\mathbb{Z}}$	$R^{\mathbb{Z}/2\mathbb{Z}}$	$T^{\mathbb{Z}/2\mathbb{Z}}$
K_3	$6L^{\mathbb{Z}/2\mathbb{Z}}$	$3L^{\mathbb{Z}/2\mathbb{Z}}$	$6F_0^{\mathbb{Z}/2\mathbb{Z}}$	$2L^{\mathbb{Z}/2\mathbb{Z}}$	$3F_0^{\mathbb{Z}/2\mathbb{Z}}$	$2F_0^{\mathbb{Z}/2\mathbb{Z}}$	$L^{\mathbb{Z}/2\mathbb{Z}}$	$F_0^{\mathbb{Z}/2\mathbb{Z}}$	$3L^{\mathbb{Z}/2\mathbb{Z}}$	$3F_0^{\mathbb{Z}/2\mathbb{Z}}$	$L^{\mathbb{Z}/2\mathbb{Z}}$	$F_0^{\mathbb{Z}/2\mathbb{Z}}$
K_5	$2T^{\mathbb{Z}/2\mathbb{Z}}$	$T^{\mathbb{Z}/2\mathbb{Z}}$	$2R^{\mathbb{Z}/2\mathbb{Z}}$	$6T^{\mathbb{Z}/2\mathbb{Z}}$	$R^{\mathbb{Z}/2\mathbb{Z}}$	$6R^{\mathbb{Z}/2\mathbb{Z}}$	$3T^{\mathbb{Z}/2\mathbb{Z}}$	$3R^{\mathbb{Z}/2\mathbb{Z}}$	$T^{\mathbb{Z}/2\mathbb{Z}}$	$R^{\mathbb{Z}/2\mathbb{Z}}$	$3T^{\mathbb{Z}/2\mathbb{Z}}$	$3R^{\mathbb{Z}/2\mathbb{Z}}$
$K_{6,0}$	$3L^{\mathbb{Z}/2\mathbb{Z}}$	$3L^{\mathbb{Z}/2\mathbb{Z}}$	$3F_0^{\mathbb{Z}/2\mathbb{Z}}$	$L^{\mathbb{Z}/2\mathbb{Z}}$	$3F_0^{\mathbb{Z}/2\mathbb{Z}}$	$F_0^{\mathbb{Z}/2\mathbb{Z}}$	$2L^{\mathbb{Z}/2\mathbb{Z}}$	$2F_0^{\mathbb{Z}/2\mathbb{Z}}$	$F_0^{\mathbb{Z}/2\mathbb{Z}} + L^{\mathbb{Z}/2\mathbb{Z}}$	$F_0^{\mathbb{Z}/2\mathbb{Z}} + L^{\mathbb{Z}/2\mathbb{Z}}$	$F_0^{\mathbb{Z}/2\mathbb{Z}}$	$L^{\mathbb{Z}/2\mathbb{Z}}$
K_7	$2L^{\mathbb{Z}/2\mathbb{Z}}$	$L^{\mathbb{Z}/2\mathbb{Z}}$	$2F_0^{\mathbb{Z}/2\mathbb{Z}}$	$6L^{\mathbb{Z}/2\mathbb{Z}}$	$F_0^{\mathbb{Z}/2\mathbb{Z}}$	$6F_0^{\mathbb{Z}/2\mathbb{Z}}$	$3L^{\mathbb{Z}/2\mathbb{Z}}$	$3F_0^{\mathbb{Z}/2\mathbb{Z}}$	$L^{\mathbb{Z}/2\mathbb{Z}}$	$F_0^{\mathbb{Z}/2\mathbb{Z}}$	$3L^{\mathbb{Z}/2\mathbb{Z}}$	$3F_0^{\mathbb{Z}/2\mathbb{Z}}$
K_8	$T^{\mathbb{Z}/2\mathbb{Z}}$	$2T^{\mathbb{Z}/2\mathbb{Z}}$	$R^{\mathbb{Z}/2\mathbb{Z}}$	$3T^{\mathbb{Z}/2\mathbb{Z}}$	$2R^{\mathbb{Z}/2\mathbb{Z}}$	$3R^{\mathbb{Z}/2\mathbb{Z}}$	$3T^{\mathbb{Z}/2\mathbb{Z}}$	$3R^{\mathbb{Z}/2\mathbb{Z}}$	$R^{\mathbb{Z}/2\mathbb{Z}}$	$T^{\mathbb{Z}/2\mathbb{Z}}$	$R^{\mathbb{Z}/2\mathbb{Z}} + T^{\mathbb{Z}/2\mathbb{Z}}$	$R^{\mathbb{Z}/2\mathbb{Z}} + T^{\mathbb{Z}/2\mathbb{Z}}$
$K_{10,0}$	$L^{\mathbb{Z}/2\mathbb{Z}}$	$2L^{\mathbb{Z}/2\mathbb{Z}}$	$F_0^{\mathbb{Z}/2\mathbb{Z}}$	$3L^{\mathbb{Z}/2\mathbb{Z}}$	$2F_0^{\mathbb{Z}/2\mathbb{Z}}$	$3F_0^{\mathbb{Z}/2\mathbb{Z}}$	$3L^{\mathbb{Z}/2\mathbb{Z}}$	$3F_0^{\mathbb{Z}/2\mathbb{Z}}$	$F_0^{\mathbb{Z}/2\mathbb{Z}}$	$L^{\mathbb{Z}/2\mathbb{Z}}$	$F_0^{\mathbb{Z}/2\mathbb{Z}} + L^{\mathbb{Z}/2\mathbb{Z}}$	$F_0^{\mathbb{Z}/2\mathbb{Z}} + L^{\mathbb{Z}/2\mathbb{Z}}$
K_4	$3T^{\mathbb{Z}/2\mathbb{Z}}$	$L^{\mathbb{Z}/2\mathbb{Z}} + T^{\mathbb{Z}/2\mathbb{Z}}$	$3R^{\mathbb{Z}/2\mathbb{Z}}$	$T^{\mathbb{Z}/2\mathbb{Z}}$	$F_0^{\mathbb{Z}/2\mathbb{Z}} + R^{\mathbb{Z}/2\mathbb{Z}}$	$R^{\mathbb{Z}/2\mathbb{Z}}$	$L^{\mathbb{Z}/2\mathbb{Z}}$	$F_0^{\mathbb{Z}/2\mathbb{Z}}$	$X_1^{\mathbb{Z}/2\mathbb{Z}} + T^{\mathbb{Z}/2\mathbb{Z}}$	$F_1^{\mathbb{Z}/2\mathbb{Z}} + R^{\mathbb{Z}/2\mathbb{Z}}$	$X_1^{\mathbb{Z}/2\mathbb{Z}}$	$F_1^{\mathbb{Z}/2\mathbb{Z}}$
$K_{6,1}$	$3L^{\mathbb{Z}/2\mathbb{Z}}$	$L^{\mathbb{Z}/2\mathbb{Z}} + T^{\mathbb{Z}/2\mathbb{Z}}$	$3F_0^{\mathbb{Z}/2\mathbb{Z}}$	$L^{\mathbb{Z}/2\mathbb{Z}}$	$F_0^{\mathbb{Z}/2\mathbb{Z}} + R^{\mathbb{Z}/2\mathbb{Z}}$	$F_0^{\mathbb{Z}/2\mathbb{Z}}$	$T^{\mathbb{Z}/2\mathbb{Z}}$	$R^{\mathbb{Z}/2\mathbb{Z}}$	$F_1^{\mathbb{Z}/2\mathbb{Z}} + L^{\mathbb{Z}/2\mathbb{Z}}$	$F_0^{\mathbb{Z}/2\mathbb{Z}} + X_1^{\mathbb{Z}/2\mathbb{Z}}$	$F_1^{\mathbb{Z}/2\mathbb{Z}}$	$X_1^{\mathbb{Z}/2\mathbb{Z}}$
K_9	$T^{\mathbb{Z}/2\mathbb{Z}}$	$L^{\mathbb{Z}/2\mathbb{Z}}$	$R^{\mathbb{Z}/2\mathbb{Z}}$	$3T^{\mathbb{Z}/2\mathbb{Z}}$	$F_0^{\mathbb{Z}/2\mathbb{Z}}$	$3R^{\mathbb{Z}/2\mathbb{Z}}$	$L^{\mathbb{Z}/2\mathbb{Z}} + T^{\mathbb{Z}/2\mathbb{Z}}$	$F_0^{\mathbb{Z}/2\mathbb{Z}} + R^{\mathbb{Z}/2\mathbb{Z}}$	$X_1^{\mathbb{Z}/2\mathbb{Z}}$	$F_1^{\mathbb{Z}/2\mathbb{Z}}$	$X_1^{\mathbb{Z}/2\mathbb{Z}} + T^{\mathbb{Z}/2\mathbb{Z}}$	$F_1^{\mathbb{Z}/2\mathbb{Z}} + R^{\mathbb{Z}/2\mathbb{Z}}$
$K_{10,1}$	$L^{\mathbb{Z}/2\mathbb{Z}}$	$T^{\mathbb{Z}/2\mathbb{Z}}$	$F_0^{\mathbb{Z}/2\mathbb{Z}}$	$3L^{\mathbb{Z}/2\mathbb{Z}}$	$R^{\mathbb{Z}/2\mathbb{Z}}$	$3F_0^{\mathbb{Z}/2\mathbb{Z}}$	$L^{\mathbb{Z}/2\mathbb{Z}} + T^{\mathbb{Z}/2\mathbb{Z}}$	$F_0^{\mathbb{Z}/2\mathbb{Z}} + R^{\mathbb{Z}/2\mathbb{Z}}$	$F_1^{\mathbb{Z}/2\mathbb{Z}}$	$X_1^{\mathbb{Z}/2\mathbb{Z}}$	$F_1^{\mathbb{Z}/2\mathbb{Z}} + L^{\mathbb{Z}/2\mathbb{Z}}$	$F_0^{\mathbb{Z}/2\mathbb{Z}} + X_1^{\mathbb{Z}/2\mathbb{Z}}$

Table 7: Domain wall fusion tables for $\mathbf{Vec}(S_3)|\mathbf{Vec}(\mathbb{Z}/2\mathbb{Z})$ domain walls with $\mathbf{Vec}(\mathbb{Z}/2\mathbb{Z})|\mathbf{Vec}(S_3)$ domain walls. Red color indicates domain walls that do not factor through vacuum.

$\otimes \text{Vec}(\mathbb{Z}/3\mathbb{Z})$	Q_1	Q_2	Q_3	Q_4	Q_5	Q_6	Q_7	$Q_{9,0}$	Q_8	$Q_{9,1}$
Q_1	$3T$	$3R_2$	$3R_3$	T	$3R$	R_2	R	R_3	T	R_3
Q_2	$3L_2$	$3A_{2,0}$	$3B_{23}$	L_2	$3D_{R,0}$	$A_{2,0}$	$D_{R,0}$	B_{23}	L_2	B_{23}
Q_3	$3L_3$	$3B_{32}$	$3A_{3,0}$	L_3	$3E_R$	B_{32}	E_R	$A_{3,0}$	L_3	$A_{3,0}$
Q_4	T	R_2	R_3	$3T$	R	$3R_2$	$3R$	$3R_3$	R_3	T
Q_5	$3L$	$3D_{L,0}$	$3E_L$	L	$3F_0$	$D_{L,0}$	F_0	E_L	L	E_L
Q_6	L_2	$A_{2,0}$	B_{23}	$3L_2$	$D_{R,0}$	$3A_{2,0}$	$3D_{R,0}$	$3B_{23}$	B_{23}	L_2
Q_7	L	$D_{L,0}$	E_L	$3L$	F_0	$3D_{L,0}$	$3F_0$	$3E_L$	E_L	L
$Q_{9,0}$	L_3	B_{32}	$A_{3,0}$	$3L_3$	E_R	$3B_{32}$	$3E_R$	$3A_{3,0}$	$A_{3,0}$	L_3
Q_8	T	R_2	R_3	L_3	R	B_{32}	E_R	$A_{3,0}$	I_3	$A_{3,1}$
$Q_{9,1}$	L_3	B_{32}	$A_{3,0}$	T	E_R	R_2	R	R_3	$A_{3,1}$	I_3

$\otimes \text{Vec}(S_3)$	Q_1	Q_2	Q_3	Q_4	Q_5	Q_6	Q_7	$Q_{9,0}$	Q_8	$Q_{9,1}$
Q_1	$6T^{\mathbb{Z}/3\mathbb{Z}}$	$3T^{\mathbb{Z}/3\mathbb{Z}}$	$2T^{\mathbb{Z}/3\mathbb{Z}}$	$6R^{\mathbb{Z}/3\mathbb{Z}}$	$T^{\mathbb{Z}/3\mathbb{Z}}$	$3R^{\mathbb{Z}/3\mathbb{Z}}$	$R^{\mathbb{Z}/3\mathbb{Z}}$	$2R^{\mathbb{Z}/3\mathbb{Z}}$	$2T^{\mathbb{Z}/3\mathbb{Z}}$	$2R^{\mathbb{Z}/3\mathbb{Z}}$
Q_2	$3T^{\mathbb{Z}/3\mathbb{Z}}$	$3T^{\mathbb{Z}/3\mathbb{Z}}$	$T^{\mathbb{Z}/3\mathbb{Z}}$	$3R^{\mathbb{Z}/3\mathbb{Z}}$	$2T^{\mathbb{Z}/3\mathbb{Z}}$	$3R^{\mathbb{Z}/3\mathbb{Z}}$	$2R^{\mathbb{Z}/3\mathbb{Z}}$	$R^{\mathbb{Z}/3\mathbb{Z}}$	$T^{\mathbb{Z}/3\mathbb{Z}}$	$R^{\mathbb{Z}/3\mathbb{Z}}$
Q_3	$2T^{\mathbb{Z}/3\mathbb{Z}}$	$T^{\mathbb{Z}/3\mathbb{Z}}$	$6T^{\mathbb{Z}/3\mathbb{Z}}$	$2R^{\mathbb{Z}/3\mathbb{Z}}$	$3T^{\mathbb{Z}/3\mathbb{Z}}$	$R^{\mathbb{Z}/3\mathbb{Z}}$	$3R^{\mathbb{Z}/3\mathbb{Z}}$	$6R^{\mathbb{Z}/3\mathbb{Z}}$	$2R^{\mathbb{Z}/3\mathbb{Z}}$	$2T^{\mathbb{Z}/3\mathbb{Z}}$
Q_4	$6L^{\mathbb{Z}/3\mathbb{Z}}$	$3L^{\mathbb{Z}/3\mathbb{Z}}$	$2L^{\mathbb{Z}/3\mathbb{Z}}$	$6F_0^{\mathbb{Z}/3\mathbb{Z}}$	$L^{\mathbb{Z}/3\mathbb{Z}}$	$3F_0^{\mathbb{Z}/3\mathbb{Z}}$	$F_0^{\mathbb{Z}/3\mathbb{Z}}$	$2F_0^{\mathbb{Z}/3\mathbb{Z}}$	$2L^{\mathbb{Z}/3\mathbb{Z}}$	$2F_0^{\mathbb{Z}/3\mathbb{Z}}$
Q_5	$T^{\mathbb{Z}/3\mathbb{Z}}$	$2T^{\mathbb{Z}/3\mathbb{Z}}$	$3T^{\mathbb{Z}/3\mathbb{Z}}$	$R^{\mathbb{Z}/3\mathbb{Z}}$	$3T^{\mathbb{Z}/3\mathbb{Z}}$	$2R^{\mathbb{Z}/3\mathbb{Z}}$	$3R^{\mathbb{Z}/3\mathbb{Z}}$	$3R^{\mathbb{Z}/3\mathbb{Z}}$	$R^{\mathbb{Z}/3\mathbb{Z}}$	$T^{\mathbb{Z}/3\mathbb{Z}}$
Q_6	$3L^{\mathbb{Z}/3\mathbb{Z}}$	$3L^{\mathbb{Z}/3\mathbb{Z}}$	$L^{\mathbb{Z}/3\mathbb{Z}}$	$3F_0^{\mathbb{Z}/3\mathbb{Z}}$	$2L^{\mathbb{Z}/3\mathbb{Z}}$	$3F_0^{\mathbb{Z}/3\mathbb{Z}}$	$2F_0^{\mathbb{Z}/3\mathbb{Z}}$	$F_0^{\mathbb{Z}/3\mathbb{Z}}$	$L^{\mathbb{Z}/3\mathbb{Z}}$	$F_0^{\mathbb{Z}/3\mathbb{Z}}$
Q_7	$L^{\mathbb{Z}/3\mathbb{Z}}$	$2L^{\mathbb{Z}/3\mathbb{Z}}$	$3L^{\mathbb{Z}/3\mathbb{Z}}$	$F_0^{\mathbb{Z}/3\mathbb{Z}}$	$3L^{\mathbb{Z}/3\mathbb{Z}}$	$2F_0^{\mathbb{Z}/3\mathbb{Z}}$	$3F_0^{\mathbb{Z}/3\mathbb{Z}}$	$3F_0^{\mathbb{Z}/3\mathbb{Z}}$	$F_0^{\mathbb{Z}/3\mathbb{Z}}$	$L^{\mathbb{Z}/3\mathbb{Z}}$
$Q_{9,0}$	$2L^{\mathbb{Z}/3\mathbb{Z}}$	$L^{\mathbb{Z}/3\mathbb{Z}}$	$6L^{\mathbb{Z}/3\mathbb{Z}}$	$2F_0^{\mathbb{Z}/3\mathbb{Z}}$	$3L^{\mathbb{Z}/3\mathbb{Z}}$	$F_0^{\mathbb{Z}/3\mathbb{Z}}$	$3F_0^{\mathbb{Z}/3\mathbb{Z}}$	$6F_0^{\mathbb{Z}/3\mathbb{Z}}$	$2F_0^{\mathbb{Z}/3\mathbb{Z}}$	$2L^{\mathbb{Z}/3\mathbb{Z}}$
Q_8	$2T^{\mathbb{Z}/3\mathbb{Z}}$	$T^{\mathbb{Z}/3\mathbb{Z}}$	$2L^{\mathbb{Z}/3\mathbb{Z}}$	$2R^{\mathbb{Z}/3\mathbb{Z}}$	$L^{\mathbb{Z}/3\mathbb{Z}}$	$R^{\mathbb{Z}/3\mathbb{Z}}$	$F_0^{\mathbb{Z}/3\mathbb{Z}}$	$2F_0^{\mathbb{Z}/3\mathbb{Z}}$	$X_1^{\mathbb{Z}/3\mathbb{Z}} + X_2^{\mathbb{Z}/3\mathbb{Z}}$	$F_1^{\mathbb{Z}/3\mathbb{Z}} + F_2^{\mathbb{Z}/3\mathbb{Z}}$
$Q_{9,1}$	$2L^{\mathbb{Z}/3\mathbb{Z}}$	$L^{\mathbb{Z}/3\mathbb{Z}}$	$2T^{\mathbb{Z}/3\mathbb{Z}}$	$2F_0^{\mathbb{Z}/3\mathbb{Z}}$	$T^{\mathbb{Z}/3\mathbb{Z}}$	$F_0^{\mathbb{Z}/3\mathbb{Z}}$	$R^{\mathbb{Z}/3\mathbb{Z}}$	$2R^{\mathbb{Z}/3\mathbb{Z}}$	$F_1^{\mathbb{Z}/3\mathbb{Z}} + F_2^{\mathbb{Z}/3\mathbb{Z}}$	$X_1^{\mathbb{Z}/3\mathbb{Z}} + X_2^{\mathbb{Z}/3\mathbb{Z}}$

Table 8: Domain wall fusion tables for $\text{Vec}(S_3)|\text{Vec}(\mathbb{Z}/3\mathbb{Z})$ domain walls with $\text{Vec}(\mathbb{Z}/3\mathbb{Z})|\text{Vec}(S_3)$ domain walls. Blue color indicates domain walls that do factor through vacuum.

$\otimes \text{Vec}(S_3)$	T	R_2	R_3	R	L_2	$A_{2,0}$	B_{23}	$D_{\pi,0}$	L_3	B_{22}	$A_{3,0}$	E_{π}	L	$D_{L,0}$	E_L	F_0	I_2	$A_{2,1}$	C_{π}	$D_{\pi,1}$	C_L	$D_{L,1}$	G_0	F_1	I_3	$A_{3,1}$	I	G_1
T	6T	6R ₂	6R ₃	6R	3T	3R ₂	3R ₃	3R	2T	2R ₂	2R ₃	2R	T	2R ₂	R ₃	R	3T	3R ₂	3R ₃	3R	T	2R ₂	2R ₃	2R	2R ₃	T	T	R ₃
R_2	3T	3R ₂	3R ₃	3R	3T	3R ₂	3R ₃	3R	T	R ₂	R ₃	R	2T	2R ₂	2R ₃	2R	R_2+T	R_2+T	R_2+T	R_2+T	T	R ₂	R	R	R ₃	T	T	R ₃
R_3	2T	2R ₂	2R ₃	2R	T	R ₂	R ₃	R	6T	6R ₂	6R ₃	6R	3T	3R ₂	3R ₃	3R	T	R ₂	R ₃	R	3T	3R ₂	3R ₃	3R	2R ₃	2T	2R ₃	T
R	T	R ₂	R ₃	2T	2R ₂	2R ₃	2R ₃	2R	3T	3R ₂	3R ₃	3R	3T	3R ₂	3R ₃	3R	R_2	R_2	R_2	R_2	R_2+T	R_2+T	R_2+T	R_2+T	R_2+T	T	T	R_2
L_2	6L ₂	6A _{2,0}	6B ₂₃	6D _{\pi,0}	3L ₂	3A _{2,0}	3B ₂₃	3D _{\pi,0}	2L ₂	2A _{2,0}	2B ₂₃	2D _{\pi,0}	L ₂	2A _{2,0}	2B ₂₃	2D _{\pi,0}	3L ₂	3A _{2,0}	3B ₂₃	3D _{\pi,0}	L ₂	A _{2,0}	B ₂₃	D _{\pi,0}	2L ₂	2B ₂₃	L ₂	B ₂₃
$A_{2,0}$	3L ₂	3A _{2,0}	3B ₂₃	3D _{\pi,0}	3L ₂	3A _{2,0}	3B ₂₃	3D _{\pi,0}	L ₂	A _{2,0}	B ₂₃	D _{\pi,0}	2L ₂	2A _{2,0}	2B ₂₃	2D _{\pi,0}	$A_{2,0}+L_2$	$A_{2,0}+L_2$	$A_{2,0}+L_2$	$A_{2,0}+L_2$	L ₂	A _{2,0}	B ₂₃	D _{\pi,0}	L ₂	B ₂₃	A _{2,0}	D _{\pi,0}
B_{23}	2L ₂	2A _{2,0}	2B ₂₃	2D _{\pi,0}	L ₂	2A _{2,0}	2B ₂₃	2D _{\pi,0}	3L ₂	3A _{2,0}	3B ₂₃	3D _{\pi,0}	3L ₂	3A _{2,0}	3B ₂₃	3D _{\pi,0}	L ₂	L ₂	D _{\pi,0}	L ₂	A _{2,0}	B ₂₃	D _{\pi,0}	3L ₂	3A _{2,0}	3B ₂₃	3D _{\pi,0}	L ₂
$D_{\pi,0}$	L ₂	A _{2,0}	B ₂₃	D _{\pi,0}	2L ₂	2A _{2,0}	2B ₂₃	2D _{\pi,0}	3L ₂	3A _{2,0}	3B ₂₃	3D _{\pi,0}	3L ₂	3A _{2,0}	3B ₂₃	3D _{\pi,0}	A _{2,0}	L ₂	D _{\pi,0}	L ₂	A _{2,0}	B ₂₃	D _{\pi,0}	3L ₂	3A _{2,0}	3B ₂₃	3D _{\pi,0}	L ₂
L_3	6L ₃	6B ₂₃	6A _{3,0}	6E _{\pi}	3L ₃	3B ₂₂	3A _{3,0}	3E _{\pi}	2L ₃	2B ₂₂	2A _{3,0}	2E _{\pi}	L ₃	2B ₂₂	2A _{3,0}	2E _{\pi}	$B_{22}+L_3$	$B_{22}+L_3$	$B_{22}+L_3$	$B_{22}+L_3$	L ₃	A _{3,0}	E _{\pi}	A _{3,0}	2L ₃	2A _{3,0}	2L ₃	E _{\pi}
$A_{3,0}$	2L ₃	2B ₂₂	2A _{3,0}	2E _{\pi}	L ₃	B ₂₂	A _{3,0}	E _{\pi}	6L ₃	6B ₂₂	6A _{3,0}	6E _{\pi}	3L ₃	3B ₂₂	3A _{3,0}	3E _{\pi}	L ₃	B ₂₂	A _{3,0}	E _{\pi}	3L ₃	3B ₂₂	3A _{3,0}	3E _{\pi}	2L ₃	2A _{3,0}	2L ₃	A _{3,0}
E_{π}	L ₃	B ₂₂	A _{3,0}	E _{\pi}	2L ₃	2B ₂₂	2A _{3,0}	2E _{\pi}	3L ₃	3B ₂₂	3A _{3,0}	3E _{\pi}	3L ₃	3B ₂₂	3A _{3,0}	3E _{\pi}	$B_{22}+L_3$	$B_{22}+L_3$	$B_{22}+L_3$	$B_{22}+L_3$	L ₃	A _{3,0}	E _{\pi}	A _{3,0}	2L ₃	2A _{3,0}	2L ₃	E _{\pi}
L	6L	6D _{L,0}	6E _L	6F ₀	3L	3D _{L,0}	3E _L	3F ₀	2L	2D _{L,0}	2E _L	2F ₀	L	D _{L,0}	E _L	F ₀	3L	3D _{L,0}	3E _L	3F ₀	L	D _{L,0}	E _L	F ₀	2L	2E _L	L	E _L
$D_{L,0}$	3L	3D _{L,0}	3E _L	3F ₀	3L	3D _{L,0}	3E _L	3F ₀	L	D _{L,0}	E _L	2F ₀	2L	2D _{L,0}	2E _L	2F ₀	$L+D_{L,0}$	$L+D_{L,0}$	$L+D_{L,0}$	$L+D_{L,0}$	L	D _{L,0}	E _L	F ₀	L	L	D _{L,0}	F ₀
E_L	2L	2D _{L,0}	2E _L	2F ₀	L	D _{L,0}	E _L	F ₀	6L	6D _{L,0}	6E _L	6F ₀	3L	3D _{L,0}	3E _L	3F ₀	L	D _{L,0}	E _L	F ₀	L	D _{L,0}	E _L	F ₀	2L	2E _L	L	E _L
F_0	L	D _{L,0}	E _L	F ₀	2L	2D _{L,0}	2E _L	2F ₀	3L	3D _{L,0}	3E _L	3F ₀	3L	3D _{L,0}	3E _L	3F ₀	$L+D_{L,0}$	$L+D_{L,0}$	$L+D_{L,0}$	$L+D_{L,0}$	L	D _{L,0}	E _L	F ₀	2L	2E _L	L	F ₀
I_2	3T	3R ₂	3R ₃	3R	L_2+T	$A_{2,0}+R_2$	$B_{23}+R_3$	$R+D_{\pi,0}$	T	R ₂	R ₃	R	L ₂	A _{2,0}	B ₂₃	D _{\pi,0}	I_2+T	$A_{2,1}+R_2$	$C_{\pi}+R_3$	$R+D_{\pi,1}$	I_2	A _{2,1}	C _{\pi}	$D_{\pi,1}$	T	R ₃	I ₂	C _{\pi}
$A_{2,1}$	3L ₂	3A _{2,0}	3B ₂₃	3D _{\pi,0}	L_2+T	$A_{2,0}+R_2$	$B_{23}+R_3$	$R+D_{\pi,0}$	L ₂	A _{2,0}	B ₂₃	D _{\pi,0}	T	R ₂	R ₃	R	$A_{2,1}+L_2$	$A_{2,0}+I_2$	$B_{23}+D_{\pi,1}$	$C_{\pi}+D_{\pi,0}$	A _{2,1}	I ₂	C _{\pi}	$D_{\pi,1}$	L ₂	B ₂₃	A _{2,1}	D _{\pi,1}
C_{π}	T	R ₂	R ₃	R	L ₂	A _{2,0}	B ₂₃	D _{\pi,0}	3T	3R ₂	3R ₃	3R	L_2+T	$A_{2,0}+R_2$	$B_{23}+R_3$	$R+D_{\pi,0}$	I_2	A _{2,1}	C _{\pi}	$D_{\pi,1}$	I_2+T	$A_{2,1}+R_2$	C _{\pi}	$D_{\pi,1}$	T	R ₃	T	C _{\pi}
$D_{\pi,1}$	L ₂	A _{2,0}	B ₂₃	D _{\pi,0}	T	R ₂	R ₃	R	3L ₂	3A _{2,0}	3B ₂₃	3D _{\pi,0}	L_2+T	$A_{2,0}+R_2$	$B_{23}+R_3$	$R+D_{\pi,0}$	$A_{2,1}+L_2$	I_2	D _{\pi,1}	$A_{2,1}+L_2$	A _{2,0}	I ₂	C _{\pi}	$D_{\pi,1}$	L ₂	B ₂₃	D _{\pi,1}	A _{2,1}
C_L	3L ₃	3A _{3,0}	3B ₂₂	3E _{\pi}	$L+L_3$	$B_{22}+D_{L,0}$	$A_{3,0}+E_L$	$E_{\pi}+F_0$	L ₃	B ₂₂	A _{3,0}	E _{\pi}	L	D _{L,0}	E _L	F ₀	C_L+L_3	$B_{22}+D_{L,1}$	$A_{3,0}+G_0$	$E_{\pi}+F_1$	C_L	D _{L,1}	$E_{\pi}+F_1$	L ₃	A _{3,0}	C _L	C _L	A _{3,1}
$D_{L,1}$	3L	3D _{L,0}	3E _L	3F ₀	$L+L_3$	$B_{22}+D_{L,0}$	$A_{3,0}+E_L$	$E_{\pi}+F_0$	L	D _{L,0}	E _L	F ₀	L ₃	B ₂₂	A _{3,0}	E _{\pi}	$C_L+D_{L,0}$	$C_L+D_{L,0}$	E_L+F_1	R_0+G_0	D _{L,1}	C _L	F ₁	C _L	L	E _L	D _{L,1}	F ₁
G_0	L ₃	B ₂₂	A _{3,0}	E _{\pi}	L	D _{L,0}	E _L	F ₀	3L ₃	3B ₂₂	3A _{3,0}	3E _{\pi}	$L+L_3$	$B_{22}+D_{L,0}$	$A_{3,0}+E_L$	$E_{\pi}+F_0$	C_L	D _{L,1}	G ₀	E_L+F_1	C_L	D _{L,1}	G ₀	L	E _L	D _{L,1}	G ₀	C _L
R_1	L	D _{L,0}	E _L	F ₀	L ₃	B ₂₂	A _{3,0}	E _{\pi}	3L	3D _{L,0}	3E _L	3F ₀	$L+L_3$	$B_{22}+D_{L,0}$	$A_{3,0}+E_L$	$E_{\pi}+F_0$	D _{L,1}	C_L	G ₀	E_L+F_1	C_L	D _{L,1}	G ₀	L	E _L	D _{L,1}	F ₁	D _{L,1}
$A_{3,1}$	2T	2R ₂	2R ₃	2R	T	R ₂	R ₃	R	2L ₃	2B ₂₂	2A _{3,0}	2E _{\pi}	L ₃	B ₂₂	A _{3,0}	E _{\pi}	I_2+T	$A_{2,1}+R_2$	$C_{\pi}+R_3$	$R+D_{\pi,1}$	I_2	A _{2,1}	C _{\pi}	$D_{\pi,1}$	T	R ₃	I ₂	A _{3,1}
I_3	2L ₃	2B ₂₂	2A _{3,0}	2E _{\pi}	L ₃	B ₂₂	A _{3,0}	E _{\pi}	2T	2R ₂	2R ₃	2R	T	R ₂	R ₃	R	I_2+T	$A_{2,1}+R_2$	$C_{\pi}+R_3$	$R+D_{\pi,1}$	I_2	A _{2,1}	C _{\pi}	$D_{\pi,1}$	T	R ₃	I ₂	A _{3,1}
T	R ₂	R ₃	R	R	L ₂	A _{2,0}	B ₂₃	D _{\pi,0}	L ₃	B ₂₂	A _{3,0}	E _{\pi}	L	D _{L,0}	E _L	F ₀	I_2	A _{2,1}	C _{\pi}	$D_{\pi,1}$	C_L	D _{L,1}	G ₀	F ₁	I ₃	I	G ₁	I ₃
G_1	L ₃	B ₂₂	A _{3,0}	E _{\pi}	L	D _{L,0}	E _L	F ₀	T	R ₂	R ₃	R	L ₂	A _{2,0}	B ₂₃	D _{\pi,0}	C_L	D _{L,1}	G ₀	E_L+F_1	C_L	D _{L,1}	G ₀	F ₁	I ₃	I	G ₁	I ₃

Table 9: Domain wall fusions for $\text{Vec}(S_3)|\text{Vec}(S_3)|\text{Vec}(S_3)$ domain walls. Entries are colored according to their origin. Domain walls colored black factor as $\text{Vec}(S_3)|\text{Vec}(\mathbb{Z}/3\mathbb{Z})|\text{Vec}(S_3)$, red domain walls factor as $\text{Vec}(S_3)|\text{Vec}(\mathbb{Z}/2\mathbb{Z})|\text{Vec}(S_3)$, blue domain walls factor as $\text{Vec}(S_3)$, and green domain walls do not factor through a smaller phase.

D Vertical fusion of binary interface defects

In this appendix, we study the fusion rings of $\text{End}(\mathcal{M})$ for bimodules $\mathcal{C} \curvearrowright \mathcal{M} \curvearrowleft \mathbf{Vec}(S_3)$ that do not factor through a smaller fusion category.

D.1 $\mathbf{Vec} | \mathbf{Vec}(S_3)$ (boundaries)

The fusion categories $\text{End}(\mathcal{A}_1)$ and $\text{End}(\mathcal{A}_2)$ are equivalent to $\mathbf{Vec}(S_3)$. Using this equivalence, we denote the binary interface defects of \mathcal{A}_1 and \mathcal{A}_2 by elements of $S_3 = \{(), (12), (13), (23), (123), (132)\}$. The fusion categories $\text{End}(\mathcal{A}_3)$ and $\text{End}(\mathcal{A}_4)$ are equivalent to $\mathbf{Rep}(S_3)$. Using these equivalences, we denote the binary interface defects of \mathcal{A}_3 and \mathcal{A}_4 by irreducible representations of S_3 , labeled $1, \sigma, \psi$ for the trivial, sign and 2D representation.

\circ	$()_1$	$(123)_1$	$(132)_1$	$(12)_1$	$(13)_1$	$(23)_1$
$()_1$	$()_1$	$(123)_1$	$(132)_1$	$(12)_1$	$(13)_1$	$(23)_1$
$(123)_1$	$(123)_1$	$(132)_1$	$()_1$	$(13)_1$	$(23)_1$	$(12)_1$
$(132)_1$	$(132)_1$	$()_1$	$(123)_1$	$(23)_1$	$(12)_1$	$(13)_1$
$(12)_1$	$(12)_1$	$(23)_1$	$(13)_1$	$()_1$	$(132)_1$	$(123)_1$
$(13)_1$	$(13)_1$	$(12)_1$	$(23)_1$	$(123)_1$	$()_1$	$(132)_1$
$(23)_1$	$(23)_1$	$(13)_1$	$(12)_1$	$(132)_1$	$(123)_1$	$()_1$

$\mathbf{Vec}(S_3) \cong \text{End}(\mathcal{A}_1)$ defect composition

\circ	$()_2$	$(123)_2$	$(132)_2$	$(12)_2$	$(13)_2$	$(23)_2$
$()_2$	$()_2$	$(123)_2$	$(132)_2$	$(12)_2$	$(13)_2$	$(23)_2$
$(123)_2$	$(123)_2$	$(132)_2$	$()_2$	$(13)_2$	$(23)_2$	$(12)_2$
$(132)_2$	$(132)_2$	$()_2$	$(123)_2$	$(23)_2$	$(12)_2$	$(13)_2$
$(12)_2$	$(12)_2$	$(23)_2$	$(13)_2$	$()_2$	$(132)_2$	$(123)_2$
$(13)_2$	$(13)_2$	$(12)_2$	$(23)_2$	$(123)_2$	$()_2$	$(132)_2$
$(23)_2$	$(23)_2$	$(13)_2$	$(12)_2$	$(132)_2$	$(123)_2$	$()_2$

$\mathbf{Vec}(S_3) \cong \text{End}(\mathcal{A}_2)$ defect composition

\circ	1_3	σ_3	ψ_3
1_3	1_3	σ_3	ψ_3
σ_3	σ_3	1_3	ψ_3
ψ_3	ψ_3	ψ_3	$1_3 + \sigma_3 + \psi_3$

$\mathbf{Rep}(S_3) \cong \text{End}(\mathcal{A}_3)$ defect composition

\circ	1_4	σ_4	ψ_4
1_4	1_4	σ_4	ψ_4
σ_4	σ_4	1_4	ψ_4
ψ_4	ψ_4	ψ_4	$1_4 + \sigma_4 + \psi_4$

$\mathbf{Rep}(S_3) \cong \text{End}(\mathcal{A}_4)$ defect composition

Table 10: Vertical fusion of \mathcal{A}_i binary interface defects

D.2 $\mathbf{Vec}(\mathbb{Z}/2\mathbb{Z}) | \mathbf{Vec}(S_3)$

The endomorphism category of all 4 $\mathbf{Vec}(\mathbb{Z}/2\mathbb{Z}) | \mathbf{Vec}(S_3)$ domain walls is $\mathbf{Rep}(\mathbb{Z}/2\mathbb{Z} \times S_3)$. We identify the binary interface defects with irreducible representations of $Z_2 \times S_3$ labeled $1, 1', \sigma, \sigma', \psi, \psi'$.

\circ	1	σ	$1'$	σ'	ψ	ψ'
1	1	σ	$1'$	σ'	ψ	ψ'
σ	σ	1	σ'	$1'$	ψ	ψ'
$1'$	$1'$	σ'	1	σ	ψ'	ψ
σ'	σ'	$1'$	σ	1	ψ'	ψ
ψ	ψ	ψ	ψ'	ψ'	$1 + \sigma + \psi$	$1' + \sigma' + \psi'$
ψ'	ψ'	ψ'	ψ	ψ	$1' + \sigma' + \psi'$	$1 + \sigma + \psi$

Table 11: Vertical defect fusion for all four $\mathbf{Vec}(\mathbb{Z}/2\mathbb{Z}) | \mathbf{Vec}(S_3)$ domain walls.

D.3 $\text{Vec}(\mathbb{Z}/3\mathbb{Z}) | \text{Vec}(S_3)$

\circ	(0, 0)	(1, 0)	(2, 0)	(0, 1)	(1, 1)	(2, 1)	(0, 2)	(1, 2)	(2, 2)	σ
(0, 0)	(0, 0)	(1, 0)	(2, 0)	(0, 1)	(1, 1)	(2, 1)	(0, 2)	(1, 2)	(2, 2)	σ
(1, 0)	(1, 0)	(2, 0)	(0, 0)	(1, 1)	(2, 1)	(0, 1)	(1, 2)	(2, 2)	(0, 2)	σ
(2, 0)	(2, 0)	(0, 0)	(1, 0)	(2, 1)	(0, 1)	(1, 1)	(2, 2)	(0, 2)	(1, 2)	σ
(0, 1)	(0, 1)	(1, 1)	(2, 1)	(0, 2)	(1, 2)	(2, 2)	(0, 0)	(1, 0)	(2, 0)	σ
(1, 1)	(1, 1)	(2, 1)	(0, 1)	(1, 2)	(2, 2)	(0, 2)	(1, 0)	(2, 0)	(0, 0)	σ
(2, 1)	(2, 1)	(0, 1)	(1, 1)	(2, 2)	(0, 2)	(1, 2)	(2, 0)	(0, 0)	(1, 0)	σ
(0, 2)	(0, 2)	(1, 2)	(2, 2)	(0, 0)	(1, 0)	(2, 0)	(0, 1)	(1, 1)	(2, 1)	σ
(1, 2)	(1, 2)	(2, 2)	(0, 2)	(1, 0)	(2, 0)	(0, 0)	(1, 1)	(2, 1)	(0, 1)	σ
(2, 2)	(2, 2)	(0, 2)	(1, 2)	(2, 0)	(0, 0)	(1, 0)	(2, 1)	(0, 1)	(1, 1)	σ
σ	σ	σ	σ	σ	σ	σ	σ	σ	σ	$\sum_{g \in \mathbb{Z}/3\mathbb{Z} \times \mathbb{Z}/3\mathbb{Z}} g$

Table 12: Vertical defect fusion for both $\text{Vec}(\mathbb{Z}/3\mathbb{Z}) | \text{Vec}(S_3)$ domain walls. This is the fusion ring of a $\mathbb{Z}/3\mathbb{Z} \times \mathbb{Z}/3\mathbb{Z}$ Tambara-Yamagami fusion category. Together with Appendix F, this establishes Proposition 2.

D.4 $\text{Vec}(S_3) | \text{Vec}(S_3)$

\circ	\bar{A}	\bar{B}	\bar{C}	\bar{D}	\bar{E}	\bar{F}	\bar{G}	\bar{H}
\bar{A}	\bar{A}	\bar{B}	\bar{C}	\bar{D}	\bar{E}	\bar{F}	\bar{G}	\bar{H}
\bar{B}	\bar{B}	\bar{A}	\bar{C}	\bar{E}	\bar{D}	\bar{F}	\bar{G}	\bar{H}
\bar{C}	\bar{C}	\bar{C}	$\bar{A} + \bar{B} + \bar{C}$	$\bar{D} + \bar{E}$	$\bar{D} + \bar{E}$	$\bar{G} + \bar{H}$	$\bar{F} + \bar{H}$	$\bar{F} + \bar{G}$
\bar{D}	\bar{D}	\bar{E}	$\bar{D} + \bar{E}$	$\bar{A} + \bar{C} + \bar{F} + \bar{G} + \bar{H}$	$\bar{B} + \bar{C} + \bar{F} + \bar{G} + \bar{H}$	$\bar{D} + \bar{E}$	$\bar{D} + \bar{E}$	$\bar{D} + \bar{E}$
\bar{E}	\bar{E}	\bar{D}	$\bar{D} + \bar{E}$	$\bar{B} + \bar{C} + \bar{F} + \bar{G} + \bar{H}$	$\bar{A} + \bar{C} + \bar{F} + \bar{G} + \bar{H}$	$\bar{D} + \bar{E}$	$\bar{D} + \bar{E}$	$\bar{D} + \bar{E}$
\bar{F}	\bar{F}	\bar{F}	$\bar{G} + \bar{H}$	$\bar{D} + \bar{E}$	$\bar{D} + \bar{E}$	$\bar{A} + \bar{B} + \bar{F}$	$\bar{C} + \bar{H}$	$\bar{C} + \bar{G}$
\bar{G}	\bar{G}	\bar{G}	$\bar{F} + \bar{H}$	$\bar{D} + \bar{E}$	$\bar{D} + \bar{E}$	$\bar{C} + \bar{H}$	$\bar{A} + \bar{B} + \bar{G}$	$\bar{C} + \bar{F}$
\bar{H}	\bar{H}	\bar{H}	$\bar{F} + \bar{G}$	$\bar{D} + \bar{E}$	$\bar{D} + \bar{E}$	$\bar{C} + \bar{G}$	$\bar{C} + \bar{F}$	$\bar{A} + \bar{B} + \bar{H}$

Table 13: Vertical fusion of G_1 binary interface defects. Notice that $\text{End}(G_1) \cong Z(\text{Vec}(S_3))$.

E Fusing anyons into binary interface defects

In this appendix, we study the action of fusing anyons from the bulk into binary interface defects.

E.1 $\text{Vec} | \text{Vec}(S_3)$ (boundaries)

$\otimes \text{Vec}(S_3)$	A	B	C	D	E	F	G	H
α	α	α	2α	3β	3β	2α	2α	2α
β	β	β	2β	3α	3α	2β	2β	2β

$\mathcal{A}_1 - \mathcal{A}_2$

$\otimes \text{Vec}(S_3)$	A	B	C	D	E	F	G	H
α	α	α	2α	$\alpha + \beta + \gamma$	$\alpha + \beta + \gamma$	$\beta + \gamma$	$\beta + \gamma$	$\beta + \gamma$
β	β	β	2β	$\alpha + \beta + \gamma$	$\alpha + \beta + \gamma$	$\alpha + \gamma$	$\alpha + \gamma$	$\alpha + \gamma$
γ	γ	γ	2γ	$\alpha + \beta + \gamma$	$\alpha + \beta + \gamma$	$\alpha + \beta$	$\alpha + \beta$	$\alpha + \beta$

$\mathcal{A}_1 - \mathcal{A}_3$

$\otimes \text{Vec}(S_3)$	A	B	C	D	E	F	G	H
α	α	α	$\beta + \gamma$	$\alpha + \beta + \gamma$	$\alpha + \beta + \gamma$	2α	$\beta + \gamma$	$\beta + \gamma$
β	β	β	$\alpha + \gamma$	$\alpha + \beta + \gamma$	$\alpha + \beta + \gamma$	2β	$\alpha + \gamma$	$\alpha + \gamma$
γ	γ	γ	$\alpha + \beta$	$\alpha + \beta + \gamma$	$\alpha + \beta + \gamma$	2γ	$\alpha + \beta$	$\alpha + \beta$

$\mathcal{A}_2 - \mathcal{A}_4$

$\otimes \text{Vec}(S_3)$	A	B	C	D	E	F	G	H
α	α	α	2α	3α	3α	2α	2α	2α

$\mathcal{A}_1 - \mathcal{A}_4$

$\otimes \text{Vec}(S_3)$	A	B	C	D	E	F	G	H
α	α	α	2α	3α	3α	2α	2α	2α

$\mathcal{A}_2 - \mathcal{A}_3$

$\otimes \text{Vec}(S_3)$	A	B	C	D	E	F	G	H
α	α	β	$\alpha + \beta$	$2\alpha + \beta$	$\alpha + 2\beta$	$\alpha + \beta$	$\alpha + \beta$	$\alpha + \beta$
β	β	α	$\alpha + \beta$	$\alpha + 2\beta$	$2\alpha + \beta$	$\alpha + \beta$	$\alpha + \beta$	$\alpha + \beta$

$\mathcal{A}_3 - \mathcal{A}_4$

Table 14: Action of S_3 anyons on defects occurring at interfaces between boundary types (corners).

The (right) action of the $\text{Vec}(S_3)$ symmetry on the boundaries is

$$\begin{aligned}
 \mathcal{A}_1 &\xleftarrow{G_1} \mathcal{A}_2 \\
 \mathcal{A}_3 &\xleftarrow{G_1} \mathcal{A}_4
 \end{aligned}
 \tag{93}$$

E.2 $\text{Vec}(\mathbb{Z}/2\mathbb{Z})|\text{Vec}(S_3)$

$\otimes \text{Vec}(\mathbb{Z}/2\mathbb{Z})$	α	$e\alpha$	αF
1	α	$e\alpha$	αF
e	$e\alpha$	α	αF
m	α	$e\alpha$	αF
em	$e\alpha$	α	αF

$K_4 - K_{6,1}$

$\otimes \text{Vec}(S_3)$	A	B	C	D	E	F	G	H
α	α	$e\alpha$	$\alpha + e\alpha$	$\alpha F + e\alpha$	$\alpha + \alpha F$	αF	αF	αF
$e\alpha$	$e\alpha$	α	$\alpha + e\alpha$	$\alpha + \alpha F$	$\alpha F + e\alpha$	αF	αF	αF
αF	αF	αF	$2\alpha F$	$\alpha + 2\alpha F + e\alpha$	$\alpha + 2\alpha F + e\alpha$	$\alpha + \alpha F + e\alpha$	$\alpha + \alpha F + e\alpha$	$\alpha + \alpha F + e\alpha$

$K_4 - K_{6,1}$

$\otimes \text{Vec}(\mathbb{Z}/2\mathbb{Z})$	α	$e\alpha$	$m\alpha$	$em\alpha$
1	α	$e\alpha$	$m\alpha$	$em\alpha$
e	$e\alpha$	α	$em\alpha$	$m\alpha$
m	$m\alpha$	$em\alpha$	α	$e\alpha$
em	$em\alpha$	$m\alpha$	$e\alpha$	α

$K_4 - K_9$

$\otimes \text{Vec}(S_3)$	A	B	C	D	E	F	G	H
α	α	$e\alpha$	$\alpha + e\alpha$	$2em\alpha + m\alpha$	$em\alpha + 2m\alpha$	$\alpha + e\alpha$	$\alpha + e\alpha$	$\alpha + e\alpha$
$e\alpha$	$e\alpha$	α	$\alpha + e\alpha$	$em\alpha + 2m\alpha$	$2em\alpha + m\alpha$	$\alpha + e\alpha$	$\alpha + e\alpha$	$\alpha + e\alpha$
$m\alpha$	$m\alpha$	$em\alpha$	$em\alpha + m\alpha$	$\alpha + 2e\alpha$	$2\alpha + e\alpha$	$em\alpha + m\alpha$	$em\alpha + m\alpha$	$em\alpha + m\alpha$
$em\alpha$	$em\alpha$	$m\alpha$	$em\alpha + m\alpha$	$2\alpha + e\alpha$	$\alpha + 2e\alpha$	$em\alpha + m\alpha$	$em\alpha + m\alpha$	$em\alpha + m\alpha$

$K_4 - K_9$

$\otimes \text{Vec}(\mathbb{Z}/2\mathbb{Z})$	α	$e\alpha$
1	α	$e\alpha$
e	$e\alpha$	α
m	α	$e\alpha$
em	$e\alpha$	α

$K_4 - K_{10,1}$

$\otimes \text{Vec}(S_3)$	A	B	C	D	E	F	G	H
α	α	$e\alpha$	$\alpha + e\alpha$	$\alpha + 2e\alpha$	$2\alpha + e\alpha$	$\alpha + e\alpha$	$\alpha + e\alpha$	$\alpha + e\alpha$
$e\alpha$	$e\alpha$	α	$\alpha + e\alpha$	$2\alpha + e\alpha$	$\alpha + 2e\alpha$	$\alpha + e\alpha$	$\alpha + e\alpha$	$\alpha + e\alpha$

$K_4 - K_{10,1}$

Table 15: Action of anyons on defects occurring at the interface of $\text{Vec}(\mathbb{Z}/2\mathbb{Z})|\text{Vec}(S_3)$ domain walls. The remaining K_i actions can be inferred using the symmetry actions of Eqn. 94

Symmetry action on the domain walls

$$\begin{array}{ccc}
 K_4 & \xleftrightarrow{G_1} & K_9 \\
 F_1 \uparrow & & \uparrow F_1 \\
 K_{6,1} & \xleftrightarrow{G_1} & K_{10,1}
 \end{array} . \quad (94)$$

E.3 $\text{Vec}(\mathbb{Z}/3\mathbb{Z})|\text{Vec}(S_3)$

$\otimes_{\text{Vec}(\mathbb{Z}/3\mathbb{Z})}$	(0,0)	(1,0)	(2,0)	(0,1)	(1,1)	(2,1)	(0,2)	(1,2)	(2,2)	σ
1	(0,0)	(1,0)	(2,0)	(0,1)	(1,1)	(2,1)	(0,2)	(1,2)	(2,2)	σ
e	(1,0)	(2,0)	(0,0)	(1,1)	(2,1)	(0,1)	(1,2)	(2,2)	(0,2)	σ
e^2	(2,0)	(0,0)	(1,0)	(2,1)	(0,1)	(1,1)	(2,2)	(0,2)	(1,2)	σ
m	(0,1)	(1,1)	(2,1)	(0,2)	(1,2)	(2,2)	(0,0)	(1,0)	(2,0)	σ
em	(1,1)	(2,1)	(0,1)	(1,2)	(2,2)	(0,2)	(1,0)	(2,0)	(0,0)	σ
e^2m	(2,1)	(0,1)	(1,1)	(2,2)	(0,2)	(1,2)	(2,0)	(0,0)	(1,0)	σ
m^2	(0,2)	(1,2)	(2,2)	(0,0)	(1,0)	(2,0)	(0,1)	(1,1)	(2,1)	σ
em^2	(1,2)	(2,2)	(0,2)	(1,0)	(2,0)	(0,0)	(1,1)	(2,1)	(0,1)	σ
e^2m^2	(2,2)	(0,2)	(1,2)	(2,0)	(0,0)	(1,0)	(2,1)	(0,1)	(1,1)	σ

$\mathbb{Z}/3\mathbb{Z}$ anyon action on both Q_8 and $Q_{9,1}$ defects

$\otimes_{\text{Vec}(S_3)}$	A	B	C	D	E	F	G	H
(0,0)	(0,0)	(0,0)	(1,0) + (2,0)	σ	σ	(1,2) + (2,1)	(0,1) + (0,2)	(1,1) + (2,2)
(1,0)	(1,0)	(1,0)	(0,0) + (2,0)	σ	σ	(0,1) + (2,2)	(1,1) + (1,2)	(0,2) + (2,1)
(2,0)	(2,0)	(2,0)	(0,0) + (1,0)	σ	σ	(0,2) + (1,1)	(2,1) + (2,2)	(0,1) + (1,2)
(0,1)	(0,1)	(0,1)	(1,1) + (2,1)	σ	σ	(1,0) + (2,2)	(0,0) + (0,2)	(1,2) + (2,0)
(1,1)	(1,1)	(1,1)	(0,1) + (2,1)	σ	σ	(0,2) + (2,0)	(1,0) + (1,2)	(0,0) + (2,2)
(2,1)	(2,1)	(2,1)	(0,1) + (1,1)	σ	σ	(0,0) + (1,2)	(2,0) + (2,2)	(0,2) + (1,0)
(0,2)	(0,2)	(0,2)	(1,2) + (2,2)	σ	σ	(1,1) + (2,0)	(0,0) + (0,1)	(1,0) + (2,1)
(1,2)	(1,2)	(1,2)	(0,2) + (2,2)	σ	σ	(0,0) + (2,1)	(1,0) + (1,1)	(0,1) + (2,0)
(2,2)	(2,2)	(2,2)	(0,2) + (1,2)	σ	σ	(0,1) + (1,0)	(2,0) + (2,1)	(0,0) + (1,1)
σ	σ	σ	2σ	$\sum g$	$\sum g$	2σ	2σ	2σ

S_3 anyon action on Q_8 defects

$\otimes_{\text{Vec}(\mathbb{Z}/3\mathbb{Z})}$	α	$e\alpha$	$e^2\alpha$	β	$e\beta$	$e^2\beta$
1	α	$e\alpha$	$e^2\alpha$	β	$e\beta$	$e^2\beta$
e	$e\alpha$	$e^2\alpha$	α	$e\beta$	$e^2\beta$	β
e^2	$e^2\alpha$	α	$e\alpha$	$e^2\beta$	β	$e\beta$
m	α	$e\alpha$	$e^2\alpha$	$e^2\beta$	β	$e\beta$
em	$e\alpha$	$e^2\alpha$	α	β	$e\beta$	$e^2\beta$
e^2m	$e^2\alpha$	α	$e\alpha$	$e\beta$	$e^2\beta$	β
m^2	α	$e\alpha$	$e^2\alpha$	$e\beta$	$e^2\beta$	β
em^2	$e\alpha$	$e^2\alpha$	α	$e^2\beta$	β	$e\beta$
e^2m^2	$e^2\alpha$	α	$e\alpha$	β	$e\beta$	$e^2\beta$

$\otimes_{\text{Vec}(S_3)}$	A	B	C	D	E	F	G	H
α	α	α	$e\alpha + e^2\alpha$	$\beta + e\beta + e^2\beta$	$\beta + e\beta + e^2\beta$	$e\alpha + e^2\alpha$	2α	$e\alpha + e^2\alpha$
$e\alpha$	$e\alpha$	$e\alpha$	$\alpha + e^2\alpha$	$\beta + e\beta + e^2\beta$	$\beta + e\beta + e^2\beta$	$\alpha + e^2\alpha$	$2e\alpha$	$\alpha + e^2\alpha$
$e^2\alpha$	$e^2\alpha$	$e^2\alpha$	$\alpha + e\alpha$	$\beta + e\beta + e^2\beta$	$\beta + e\beta + e^2\beta$	$\alpha + e\alpha$	$2e^2\alpha$	$\alpha + e\alpha$
β	β	β	$e\beta + e^2\beta$	$\alpha + e\alpha + e^2\alpha$	$\alpha + e\alpha + e^2\alpha$	$e\beta + e^2\beta$	$e\beta + e^2\beta$	2β
$e\beta$	$e\beta$	$e\beta$	$\beta + e^2\beta$	$\alpha + e\alpha + e^2\alpha$	$\alpha + e\alpha + e^2\alpha$	$\beta + e^2\beta$	$\beta + e^2\beta$	$2e\beta$
$e^2\beta$	$e^2\beta$	$e^2\beta$	$\beta + e\beta$	$\alpha + e\alpha + e^2\alpha$	$\alpha + e\alpha + e^2\alpha$	$\beta + e\beta$	$\beta + e\beta$	$2e^2\beta$

Table 16: Action of anyons on defects occurring at the interface of $\text{Vec}(\mathbb{Z}/3\mathbb{Z})|\text{Vec}(S_3)$ domain walls Q_8 and $Q_{9,1}$. The remaining actions can be inferred using the symmetry actions of Eqn. 95

Symmetry action on the domain walls

$$\begin{array}{c}
 \begin{array}{ccc}
 & F_1 & \\
 X_2 \curvearrowright Q_8 & \xleftrightarrow{\quad} & Q_{9,1} \curvearrowright X_2 \\
 & G_1 &
 \end{array}
 \end{array} . \quad (95)$$

E.4 $\mathbf{Vec}(S_3)|\mathbf{Vec}(S_3)$

$\otimes \mathbf{Vec}(S_3)$	σ	$B\sigma$	$C\sigma$	ρ	$B\rho$	$C\rho$
A	σ	$B\sigma$	$C\sigma$	ρ	$B\rho$	$C\rho$
B	$B\sigma$	σ	$C\sigma$	$B\rho$	ρ	$C\rho$
C	$C\sigma$	$C\sigma$	$B\sigma + C\sigma + \sigma$	$C\rho$	$C\rho$	$B\rho + C\rho + \rho$
D	$B\rho + C\rho$	$C\rho + \rho$	$B\rho + 2C\rho + \rho$	$B\sigma + C\sigma$	$C\sigma + \sigma$	$B\sigma + 2C\sigma + \sigma$
E	$C\rho + \rho$	$B\rho + C\rho$	$B\rho + 2C\rho + \rho$	$C\sigma + \sigma$	$B\sigma + C\sigma$	$B\sigma + 2C\sigma + \sigma$
F	$C\sigma$	$C\sigma$	$B\sigma + C\sigma + \sigma$	$C\rho$	$C\rho$	$B\rho + C\rho + \rho$
G	$B\sigma + \sigma$	$B\sigma + \sigma$	$2C\sigma$	$C\rho$	$C\rho$	$B\rho + C\rho + \rho$
H	$C\sigma$	$C\sigma$	$B\sigma + C\sigma + \sigma$	$B\rho + \rho$	$B\rho + \rho$	$2C\rho$

Table 17: Action of anyons on defects occurring at the interface of the $\mathbf{Vec}(S_3)|\mathbf{Vec}(S_3)$ domain walls G_1 and I (twists).

F Associator for $\text{End}(Q_8)$

We now provide an example computation of the associator for objects in $\text{End}(Q_8)$. Recall that the left category is $\mathbf{Vec}(\mathbb{Z}/3\mathbb{Z})$ and the right category is $\mathbf{Vec}(S_3)$. A basis for the annular category representations is given by

$$\begin{array}{c} \text{Diagram with two loops } x \text{ and } (y, z) \end{array} : \begin{array}{c} (a, (1+a)h+b) \\ \text{Diagram with node } (g, h) \\ (a, b) \end{array} \mapsto \omega^{-gx} \begin{array}{c} (a+y, (1+y)((1+a)(h+x)+b)+z) \\ \text{Diagram with node } (g, h) \\ (a+y, (1+y)((1+a)x+b)+z) \end{array}, \quad (96)$$

$$\begin{array}{c} (a+1, 2b+c) \\ \text{Diagram with node } \sigma \\ (a, b) \end{array} \mapsto \begin{array}{c} (1+a+y, (1+y)(2(1+a)x+2b+c)+z) \\ \text{Diagram with node } \sigma \\ (a+y, (1+y)((1+a)x+b)+z) \end{array}, \quad (97)$$

where node labels indicate irreps, $a, y \in \{0, 1\}$, $b, c, g, h, x, z \in \{0, 1, 2\}$. We remark that at all times, the left entry of the string label should be taken modulo 2 and the right entry modulo 3.

From these representations, we construct the compound defects associated to vertical fusion. By studying the annular action on these compound defects, we obtain the following decompositions into simple defects

$$\begin{array}{c} (a, (1+a)(h_0+h_1)+b) \\ \text{Diagram with nodes } (g_1, h_1) \text{ and } (g_0, h_0) \\ (a, b) \end{array} \cong \begin{array}{c} (a, (1+a)(h_0+h_1)+b) \\ \text{Diagram with node } (g_0+g_1, h_0+h_1) \\ (a, b) \end{array}, \quad (98a)$$

$$\begin{array}{c} (a+1, 2(1+a)h+2b+c) \\ \text{Diagram with nodes } \sigma \text{ and } (g, h) \\ (a, b) \end{array} \cong \omega^{g(1+a)(b+c)+gh} \begin{array}{c} (a+1, 2(1+a)h+2b+c) \\ \text{Diagram with node } \sigma \\ (a, b) \end{array}, \quad (98b)$$

$$\begin{array}{c} (1+a, 2(1+a)h+2b+c) \\ \text{Diagram with nodes } (g, h) \text{ and } \sigma \\ (a, b) \end{array} \cong \omega^{(1+a)(b+c)g} \begin{array}{c} (a+1, 2(1+a)h+2b+c) \\ \text{Diagram with node } \sigma \\ (a, b) \end{array}, \quad (98c)$$

$$\begin{array}{c}
(a, (1+a)h+b) \\
\begin{array}{|c|} \hline \bullet \\ \hline \end{array} \\
\sigma \\
\begin{array}{|c|} \hline \bullet \\ \hline \end{array} \\
\sigma \\
(a, b)
\end{array}
\cong \frac{1}{\sqrt{3}} \sum_g \omega^{2(1+a)(b+c)g}
\begin{array}{c}
(a, (1+a)h+b) \\
\begin{array}{|c|} \hline \bullet \\ \hline \end{array} \\
(g, h) \\
(a, b)
\end{array} . \quad (98d)$$

Given these isomorphisms, the computation of the associator is straightforward. We illustrate for $(\sigma \circ \sigma) \circ \sigma = \sum_{(g_0, h_0), (g_1, h_1)} [F_{\sigma, \sigma, \sigma}^\sigma]_{(g_0, h_0), (g_1, h_1)} \sigma \circ (\sigma \circ \sigma)$.

$$\begin{array}{c}
(1+a, 2(1+a)h_1+2b+c) \\
\begin{array}{|c|} \hline \bullet \\ \hline \end{array} \\
\sigma \\
\begin{array}{|c|} \hline \bullet \\ \hline \end{array} \\
\sigma \\
\begin{array}{|c|} \hline \bullet \\ \hline \end{array} \\
\sigma \\
(a, (1+a)h_0+b) \\
(1+a, 2b+c) \\
(a, b)
\end{array}
\begin{array}{c}
\sigma \\
(g_0, h_0)
\end{array}
\begin{array}{c}
\sigma \\
\end{array}
\begin{array}{c}
\sigma \\
\end{array}
\begin{array}{c}
\omega^{2(1+a)(b+c)g_0} \\
\sqrt{3}
\end{array}
\begin{array}{c}
\omega^{(1+a)(b+c)g_0+2g_0(h_0+h_1)}
\end{array}
\quad (99)$$

$$\begin{array}{c}
(1+a, 2(1+a)h_0+2b+c_1) \\
\begin{array}{|c|} \hline \bullet \\ \hline \end{array} \\
\sigma \\
\begin{array}{|c|} \hline \bullet \\ \hline \end{array} \\
\sigma \\
\begin{array}{|c|} \hline \bullet \\ \hline \end{array} \\
\sigma \\
(a, (1+a)h_0+b) \\
(1+a, 2b+c_0) \\
(a, b)
\end{array}
\begin{array}{c}
\sigma \\
(g_1, h_1)
\end{array}
\begin{array}{c}
\sigma \\
\end{array}
\begin{array}{c}
\sigma \\
\end{array}
\begin{array}{c}
\omega^{2g_1(1+a)(b+c)+h_0g_1} \\
\sqrt{3}
\end{array}
\begin{array}{c}
\omega^{(1+a)(b+c)g_1}
\end{array}
\quad (100)$$

From this, we obtain

$$[F_{\sigma, \sigma, \sigma}^\sigma]_{(g_0, h_0), (g_1, h_1)} \text{id}_\sigma = \begin{array}{c} \sigma \\ \begin{array}{|c|} \hline \bullet \\ \hline \end{array} \\ \sigma \\ \begin{array}{|c|} \hline \bullet \\ \hline \end{array} \\ \sigma \\ \begin{array}{|c|} \hline \bullet \\ \hline \end{array} \\ \sigma \\ (g_0, h_0) \end{array} \begin{array}{c} (g_1, h_1) \\ \begin{array}{|c|} \hline \bullet \\ \hline \end{array} \\ \sigma \\ \begin{array}{|c|} \hline \bullet \\ \hline \end{array} \\ \sigma \\ \begin{array}{|c|} \hline \bullet \\ \hline \end{array} \\ \sigma \\ (g_1, h_1) \end{array} \begin{array}{c} \sigma \\ \end{array} = \frac{\omega^{2(g_1h_0+g_0(h_0+h_1))}}{3} \text{id}_\sigma . \quad (101)$$

The remaining associator elements can be found in a similar way. After regauging the trivalent vertices, we obtain

$$[F_{(g_0, h_0), \sigma, (g_1, h_1)}^\sigma]_{\sigma, \sigma} = \chi((g_0, h_0), (g_1, h_1)) \quad (102a)$$

$$[F_{\sigma, (g_0, h_0), \sigma}^{(g_1, h_1)}]_{\sigma, \sigma} = \chi((g_0, h_0), (g_1, h_1)) \quad (102b)$$

$$[F_{\sigma, \sigma, \sigma}^\sigma]_{(g_0, h_0), (g_1, h_1)} = \frac{\nu}{3\chi((g_0, h_0), (g_1, h_1))}, \quad (102c)$$

with $\nu = 1$ and $\chi()$ the symmetric bicharacter defined by

$$\chi((g_0, h_0), (g_1, h_1)) = \omega^{g_0h_1+h_0g_1}. \quad (103)$$

G $\mathbf{Vec}(\mathbb{Z}/p\mathbb{Z})$ bimodule data

In this appendix, we reproduce the defining data for $\mathbf{Vec}(\mathbb{Z}/p\mathbb{Z})$ bimodule categories. Additionally, we reproduce the Brauer-Picard tables for these bimodules and physical interpretations.

Bimodule label	Left action	Right action	Associator
T	$(a+g, b)$ 	$(a, b+g)$ 	$(a+g, b+h) = (a+g, b+h)$
L	a 	$a+g$ 	$a+h$
R	$g+a$ 	a 	$g+a$
F_0	$*$ 	$*$ 	$*$
X_k	$a+g$ 	$a+kg$ 	$g+a+kh = g+a+kh$
F_q	$*$ 	$*$ 	$= e^{\frac{2\pi i}{p} qgh}$

Table 18: Data for all $\mathbf{Vec}(\mathbb{Z}/p\mathbb{Z}) - \mathbf{Vec}(\mathbb{Z}/p\mathbb{Z})$ bimodules. $q \in H^2(\mathbb{Z}/p\mathbb{Z}, U(1)) \cong \mathbb{Z}/p\mathbb{Z}$. Bimodules below the thick line are invertible. Note that in the main text, these bimodule labels are supplemented with a superscript indicating for which $\mathbf{Vec}(\mathbb{Z}/p\mathbb{Z})$ they are defined. Reproduced from Ref. [34].

$\otimes \mathbf{Vec}(\mathbb{Z}/p\mathbb{Z})$	T	L	R	F_0	X_l	F_r
T	$p \cdot T$	T	$p \cdot R$	R	T	R
L	$p \cdot L$	L	$p \cdot F_0$	F_0	L	F_0
R	T	$p \cdot T$	R	$p \cdot R$	R	T
F_0	L	$p \cdot L$	F_0	$p \cdot F_0$	F_0	L
X_k	T	L	R	F_0	X_{kl}	$F_{k^{-1}r}$
F_q	L	T	F_0	R	F_{ql}	$X_{q^{-1}r}$

Table 19: Multiplication table for $\mathbf{BPR}(\mathbf{Vec}(\mathbb{Z}/p\mathbb{Z}))$, reproduced from Ref. [34].







Bimodule label	Domain wall	Action on particles
T		Condenses e on both sides
L		Condenses m on left and e on right
R		Condenses e on left and m on right
F_0		Condenses m on both sides
X_k		$X_k : e^a m^b \mapsto e^{ka} m^{k^{-1}b}$
$F_q = F_1 X_q$		$F_1 : e^a m^b \mapsto e^b m^a$

Table 20: Domain walls on the lattice corresponding to bimodules. Reproduced from Ref. [34].